Master's thesis

NTNU
Norwegian University of Science and Technology
Faculty of Information Technology and Electrical Engineering
Department of Engineering Cybernetics

Truls Kjøsnes Olsen

Modeling and Analysis of a Dynamic Positioning System for a Wave Energy Converter

Master's thesis in Engineering Cybernetics
Supervisor: Morten D. Pedersen
June 2021

NTNU
Norwegian University of
Science and Technology

Truls Kjøsnes Olsen

Modeling and Analysis of a Dynamic Positioning System for a Wave Energy Converter

Master's thesis in Engineering Cybernetics
Supervisor: Morten D. Pedersen
June 2021

Norwegian University of Science and Technology
Faculty of Information Technology and Electrical Engineering
Department of Engineering Cybernetics

NTNU
Norwegian University of
Science and Technology

Abstract

Waveco is developing a new wave energy converter with two components, an underwater turbine attached to a buoy on the ocean surface that floats in the waves. The buoy's motion then moves the turbine up and down deep below the wave zone, generating power.

However, there are concerns about ocean currents affecting the turbine dragging the turbine away from its wanted position under the buoy. In this thesis, a nonlinear model is developed for the wave energy converter to characterize stability and provide recommendations for the aforementioned highly nonlinear and adverse effects on the system.

The model is Lagrangian based, with hydrodynamical forces modeled with Morison equations in both heave and surge, and the inertia force is integrated across the submerged volume of the buoy. Control force is then generated with a set of wings attached to the turbine. A linear model is developed to design a Linear quadratic regulator to control the force generated from the wings to steer the turbine back to its wanted position. The model is simulated with realistic conditions using numerical simulation to study the feasibility of the system.

Sammendrag

Waveco utvikler et nytt type bølgekraftverk bestående av to deler, en undervanns turbin festet til en bøye som flyter på havoverflaten og følger bølgenes bevegelse. Bøyens bevegelse beveger dermed turbinen som flyter dypt under bølgesonen og skaper dermed energi.

Det foreligger bekymringer om at havstrømmer kommer til å påvirke turbinen og dra den bort fra den ønskede posisjonen under bøyen. Denne avhandlingen utvikler en ulineær modell for bølgekraftverket for å karakterisere dets stabilitet og gi en anbefalinger for det nevnte høyst ulineære systemet og de påvirkende effektene på systemet.

Modellen er Lagrangian basert, med hydrodynamiske krefter modellert ved Morison likningene i to dimensjoner. Treghetskraften blir funnet ved hjelp av integrasjon over dent nedsenkede volumet til bøyen. Styringskraft blir skapt ved to vinger festet på turbinen. En liner modell blir utviklet for å designe en Linear Quadratic regulator, som blir bruk til å regulere styringskraften fra vingene for å styre turbinen tilbake til ønsket posisjon. Modellen blir så numerisk simulert under realistiske kondisjoner for å utforske gjennomførbarheten til systemet.

Acknowledgments

I want to thank Inge Bakke at Waveco for giving me the opportunity to work with them as a part of this thesis. It has been an exciting project to work on, and I have learned so much over this period. Seeing the knowledge gained through years of education being put to use has been very rewarding. My warmest gratitude goes to my supervisor Morten D. Pedersen, who has supported my efforts the entire way and has given me motivation and access to his deep knowledge throughout this last year.

List of Figures

Nomenclature

WAC	Wave Energy Converter
DoF	Degrees of Freedom
l	Rope length
l_b	Length from Top of Turbine to CB
l_g	Length from Top of Turbine to CG
CB	Center of Buoyancy
CG	Center of Gravity
q	Generalized Coordinates
$\boldsymbol{\gamma}$	Vector of Generalized Coordinates
J	Moment of Inertia for Turbine
T	Kinetic Energy
U	Potential Energy
Q_i	Generalized Force
m_i	Mass
ρ	Density of Water
V_t	Volume Turbine
g	Acceleration of Gravity
F_b	Buoyancy Force
F_g	Gravitational Force
SWL	Still Water Line
$\boldsymbol{D}(\gamma)$	Mass Matrix

$\boldsymbol{C}(\gamma, \dot{\gamma})$	Coriolis Matrix
$\boldsymbol{G}(\gamma)$	Stiffness Matrix
λ	Wavelength
H	Wave Height
δ_a	Wave Amplitude
k	Wavenumber
ω	Wave Angular Frequency
ϵ	Random Phase Angle
$S(\omega)$	Wave Spectrum
$\Delta\omega$	Constant Frequency Difference
JONSWAP	Joint North Sea Wave Project
H_s	Significant Wave Hight
T_0	Peak Period
T_1	Average Wave Period
T_z	Zero-Crossing Wave Period
∇_b	Volume Buoy
C_a	Added Mass Coefficient
C_d	Drag Coefficient
C_l	Lift Coefficient
F_l	Lift Force
Q_m	Generalized Morison Force
Q_d	Generalized Drag Force
Q_l	Generalized Lift Force
α_w	Angle of Attack
$\boldsymbol{\varsigma}$	State Space Vector
LQR	Linear Quadratic Regulator

Contents

Chapter 1

Introduction

The company Waveco is developing a Wave Energy Converter(WEC). However, there are concerns that the system might be affected by ocean currents that would negatively impact the system dynamics, that is, might drag the system out of position and affecting its ability to generate power optimally. Throughout this thesis, a model is built to investigate these concerns and potentially mitigate them.

1.1 Waveco's Underwater Turbine

Waveco are investigating a new approach for a WEC as they are developing an underwater turbine named Subway, intended to be used in different settings to generate power. The basic idea is that they have a long cylindrical-shaped turbine, with two sets of rotors attached to the body, as seen in figure 1.1. The two rotors are counter-rotating, and the moment generated by the rotation as water moves over the blades is used to generate power. The blades themself are flexible and are attached so that each blade always rote in the same direction.

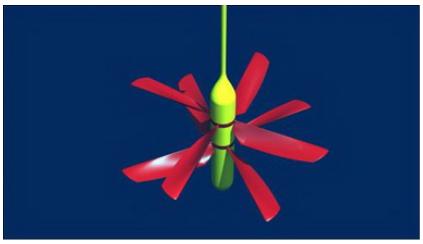

Figure 1.1: An illustration of the basic shape of the Subwave turbine. (Waveco AS)

Waveco envisions a few different applications for their turbine, including a tidal power generator, where the turbine is mounted horizontal and anchored down in place, generating power with the changing tidal currents. However, the two main uses of interest for this thesis are where it is being used in a vertical configuration. The main idea is that the turbine is attached to a floating object on the surface that follows the waves' motions, which move the turbine up and down, generating power. A ballast weighs down the turbine for stabilizing purposes and makes sure the rope connecting the turbine to the surface floater is kept tight at all times to avoid unwanted jerk forces.

In this setting, the first product envisioned by Waveco is the Automar ocean observation buoy, a self-sustaining anchoress observation platform. It is common for deepwater observation buoys to be free-floating or have expensive anchoring that increases with depth, making it hard to deploy an observation buoy that stays in the same location over a long time. The Automar buoy aims to change this by having a ready-to-deploy solution that uses a surface vessel equipped with dynamic positioning electric motors along with the array of sensors needed. The power needed to maintain the position required overtime is then provided by the attached turbine, as illustrated in figure 1.2. The turbine then charges the internal battery of the observation buoy, allowing it to stay put even when there is too low of a wave profile to generate power while at the same time providing power to the onboard sensors.

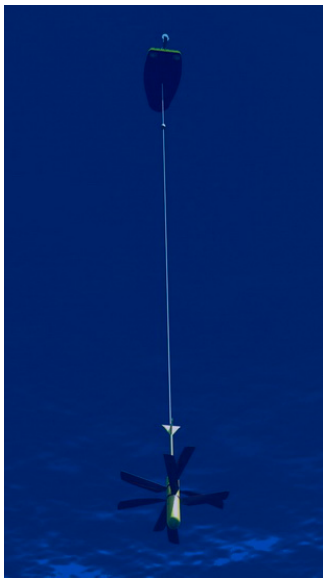

Figure 1.2: The Automar ocean observation buoy system, as seen from below, attached to the Subway turbine. (Waveco AS)

The other application turbine is a pure power generating system. It is imagined that an array of turbines are deployed off the coast, where the water is so deep that the turbine can float below the wave zone but still permits anchoring, allowing the turbine itself to avoid being affected by the wave forces, and it is commonly set in the literature as half a wavelengths depth [1]. The turbine would be floating under a buoy, with multiple moored together, and in the end, they would be attached to an anchor point. Both of these configurations are illustrated in figure 1.3. Here, a proposed idea is to combine a fleet of Subway turbines with an existing offshore wind plant, as the necessary infrastructure is already in place. It would allow the turbines to float between the wind turbines, attaching to their anchoring. This solution also gives the advantage that the ocean space is used more efficiently, considering space is a finite resource, improving the power-output per square kilometer of sea claimed.

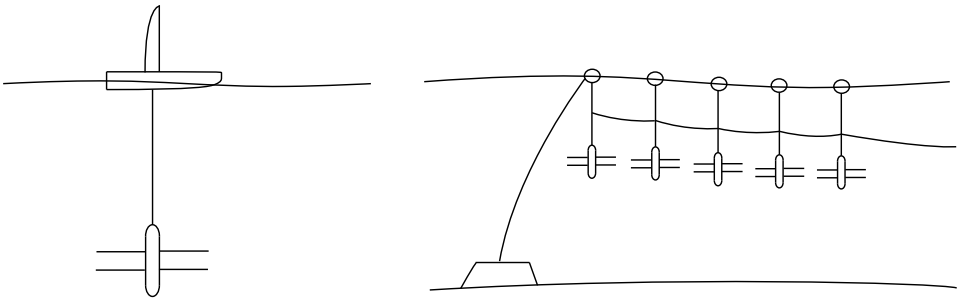

Figure 1.3: To the right the Automar buoy and the attached Subway turbine. And to the left multiple Subway systems anchored together in a power generating configuration.

1.2 Overview of Current Wave Energy Converters

There already exists a wide field of different wave energy converts in various stages of development. And the history of attempting to harness energy from waves goes as far back as the 1800s. It did not see renewed interest before the 1970s and the rising demand for new energy sources. One possible classification of WECs can be done with regards to the primary way they extract energy. There are three main groups in this classification: Oscillating water columns, Wave activated bodies and Overtopping. These can be further broken down into subclasses, but we will look at the main types briefly here [2].

Oscillating water columns work by pressure difference. They are semi-submerged and open down into the sea, where an air pocket is trapped inside a chamber connected to the outside atmosphere via a turbine. When the waves roll in, the air moves to equalize, generating power as it moves through the turbine.

Then we have wave-activated bodies, probably the largest group of WECs. This group encompasses a wide range of different shapes and ideas, but the main principle is that the wave interacts with the body of the WEC to create energy. Wavecos Subwave would fall under this category, using heave translation. Another example would be a tilting device using the surge motion of the wave to move back and forth with the motions of the wave, as illustrated in figure 1.4

Lastly, there are overtopping devices. These can be imaged as an open tank, that when waves come crashing into the sides of them, the water overflows into the chamber. The water collected then drains out through a turbine, and generating power.

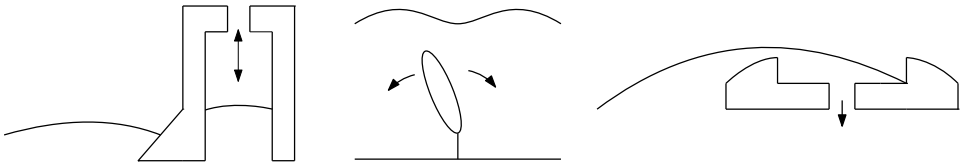

Figure 1.4: Examples of the three main types of WECs, Oscillating water columns(left), Wave activated bodies(center) and Overtopping(right)

1.3 Possible Contributions

- First-principles modeling of a novel wave energy converter Lagrangian mechanics and classical hydrodynamics.
- A modeling pipeline that could be expanded to add in more degrees of freedom and forces.
- Development and validation of an optimal control system based on a linearized model of the system.
- A study of practical feasibility under realistic conditions using numerical simulations of the nonlinear model in closed loop.
- Recommendations addressing the concerns that this thesis is based on and suggested actions.

1.4 Problem Statement and Structure

The Subwave turbine's concern is that of ocean currents. The Norwegian coastal current in the Norwegian sea has speeds as high as over 1 m/s [3], but are typically characterized by a speed of 0.3 m/s [4]. The drag generated by these speeds may cause a problem for the turbine as it might get carried away, causing sub-optimal heave motion or interfering with other equipment nearby.

This thesis aims to investigate the effect of the current on the turbine and the possibility to negate the effect of the ocean current drag with a set of control wings, generating lift force to steer the turbine back into position using the same heave motion that generates energy. The outline of the thesis will be

2. Mathematical Modelling - A few assumptions are outlined before a non-linear kinetic model is made with a Lagrangian approach, and then the forces acting on the system are added.
3. Linearization and Control - The mathematical model is then simplified and linearized, such that it is possible to develop a linear controller for the system.
4. Simulation - The different aspects of the model are thoroughly explored here, and the controller's performance is compared to a system without a controller.
5. Discussion - The model and the results of the simulations are discussed to see what could be improved upon, recommendations based on the work are presented while future work is presented.

Chapter 2

Mathematical Modelling

We start with making a few assumptions of the system that allow us to build a mathematical model to analyze the system's behavior and develop a controller later.

2.1 Assumptions

The system, as mentioned, consists of two parts, a floating surface vehicle attached to an underwater turbine with a rope. The underwater turbine is shaped in a tear-drop-like fashion to minimize ocean-current drag and has a fixed-wing at the back to ensure the turbine always aligns itself with the ocean currents, as seen in figure 2.1. There are also two controllable wings attached to the side for control purposes. Originally the intent was to have more controllable wings around the body to achieve full control in 6-DoF, as explored in the pre-thesis project. However, the added complexity of this implementation with 6 controllable wings was found too high, and Waveco put forward this simpler configuration.

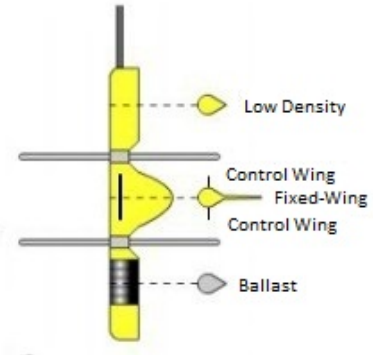

Figure 2.1: The suggested shape of the Subway turbine, with the control wings and the fixed-wing at the back. (Waveco AS)

When developing the model, a few constraints are imposed on the system to simplify derivations. By looking at the original concept, a few natural limitations can be set. We can assume that the turbine is aligning itself with the ocean current due to its shape. The two sets of turbine blades generate a slightly different moment. However, the assumption is that the fixed-wing can dampen this moment. If this is not the case, the control wings could be used to counter this moment at a later point. When describing the motion of a craft is common to talk of the 6-DoF, as shown in figure 2.2. However, due to these constraints, we can limit our model to the 2D xz-plane and 3-DoF in Surge, Heave, and Pitch.
As for the rope connecting the surface vessel and turbine, there are ways of modeling ropes as a rigid multi-body system [5]. Though, the added complexity of the model would make the overall model hard to develop. Still, it is safe to assume that the rope is held in tension for normal operating conditions as a ballast weights down the turbine, allowing the rope to be viewed as a thin massless rod. The ballast is assumed to be placed at the bottom of the turbine for a low center of gravity. The surface floater is modeled as a spherical buoy, as this allows for more straightforward hydrodynamic force calculation without affecting the overall dynamics of the system in a way that would nullify the results. The turbine propellers would add a not-insignificant amount of drag force in heave. But we are here interested in the best case for the control system, so the main drag from the turbine rotors is neglected.

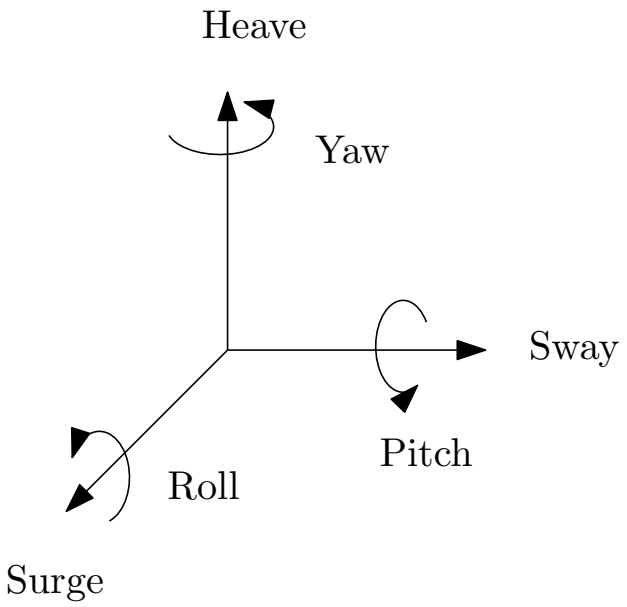

Figure 2.2: The 6 Degrees of Freedom, Surge, Heave, Sway, Roll, Pitch and Yaw.

2.2 Kinematics

As the system is connected by the rope, the motion of the turbine is constrained to a circle around the buoy with radius l. We view this as a system with 3 particles, the center of mass and center of buoyancy for the buoy coincide here are and are viewed as one particle. The other two particles are the center of buoyancy for the turbine(CB), and lastly, the center of gravity for the turbine. The turbine's CB is also the point where the forces affecting the turbine are calculated. We denominate the position of each particle as

$$\mathbf{r}_1 = \begin{bmatrix} x \\ z \end{bmatrix}, \quad \mathbf{r}_2 = \begin{bmatrix} x_{t_b} \\ z_{t_b} \end{bmatrix}, \quad \mathbf{r}_3 = \begin{bmatrix} x_{t_g} \\ z_{t_g} \end{bmatrix}. \tag{2.1}$$

If we can express the constraint by an equation on the form,

$$f(\mathbf{r}_1, \mathbf{r}_2, \mathbf{r}_3, ..., t) = 0 \tag{2.2}$$

, it is said to be a holonomic constraint, and it introduces two difficulties. Firstly, the coordinates are no longer independent, and thus the equations of motion are not. Secondly, the forces of the constraints are not known. However, both of these can be overcome by introducing generalized coordinates and choosing the Lagrangian approach [6].

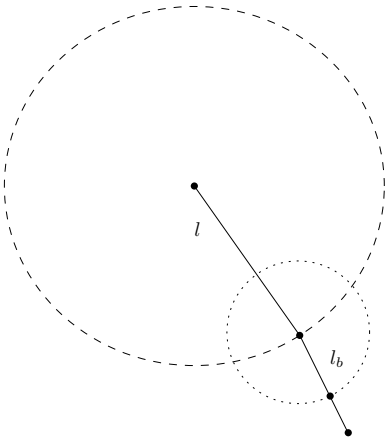

Figure 2.3: The buoy constricting the motion of the turbine in a circle with radius l

A general system of particles in the xz-plane without any constraints has 2-DoF, giving $2N$ independent coordinates. If there exist holonomic constraints on the system, we can use these k constraints to eliminate k of the variables, giving us a system of $2N - k$ coordinates. We can express this elimination of dependent coordinates in another way.

Expressing the dependent variables r with the new generalized coordinates q as

$$\begin{aligned} \mathbf{r}_1 &= \mathbf{r}_1(q_1, q_2, ..., q_{N-k}) \\ &\vdots \\ \mathbf{r}_N &= \mathbf{r}_N(q_1, q_2, ..., q_{N-k}), \end{aligned} \tag{2.3}$$

these equations then contain the constraints in them implicitly. As for the forces of constraints, they disappear by D'Alembert's principle. Leading to Lagrange's equation

$$\begin{aligned} &\frac{d}{dt}\left(\frac{\partial \mathcal{L}}{\partial \dot{q}_i}\right) - \frac{\partial \mathcal{L}}{\partial q_i} = Q_i, \\ &\mathcal{L} = T - U. \end{aligned} \tag{2.4}$$

T is the system's kinetic energy, and U is the potential energy of the system. And Q_i is the generalized forces acting on the system, defined as

$$Q_i = \sum_j F_j \cdot \frac{\partial \mathbf{r}_j}{\partial q_i}. \tag{2.5}$$

As noted and seen in figure 2.4, we can represent the system as 3 particles with 4 generalized coordinates, as we have two constraints in the motions of the particles. The generalized coordinates are then

$$\boldsymbol{\gamma} = \begin{bmatrix} x \\ z \\ \alpha \\ \theta \end{bmatrix}. \tag{2.6}$$

Expressing the positions of the particles in the form given in (2.3)

$$\mathbf{P}_0 = \begin{bmatrix} x \\ z \end{bmatrix}, \ \mathbf{P}_1 = \begin{bmatrix} x + l\sin(\alpha) + l_b\sin(\theta) \\ z - l\cos(\alpha) - l_b\cos(\theta) \end{bmatrix}, \ \mathbf{P}_2 = \begin{bmatrix} x + l\sin(\alpha) + l_g\sin(\theta) \\ z - l\cos(\alpha) - l_g\cos(\theta) \end{bmatrix}. \tag{2.7}$$

The kinetic energy of the system is then

$$T = \frac{1}{2}m_0||\dot{\mathbf{P}}_0||^2 + \frac{1}{2}m_2||\dot{\mathbf{P}}_2||^2 + \frac{1}{2}J\dot{\theta}^2, \tag{2.8}$$

J, being the moment of inertia for the turbine. The potential energy is

$$U = -\rho V_t g P_{1z} + m_2 g P_{2z}, \tag{2.9}$$

V_t is the volume of the turbine, while ρ is the density of water. Potential forces of the buoy are not considered right now but are added on later. The

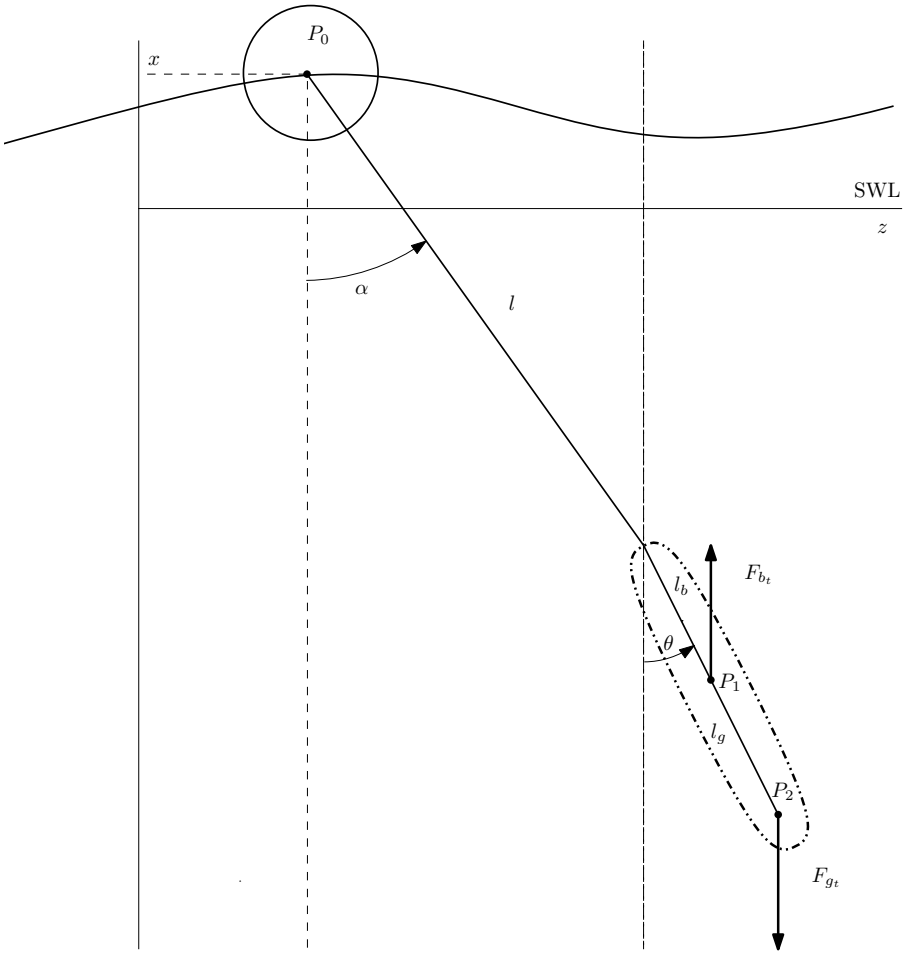

Figure 2.4: The system seen as three different particles kept together by holonomic constraints.

rope connecting the floater and the turbine is considered massless, and the moment of the buoy is ignored. The velocity of the points are found as

$$\dot{\mathbf{P}}_0 = \begin{bmatrix} \dot{x} \\ \dot{z} \end{bmatrix}, \ \dot{\mathbf{P}}_1 = \begin{bmatrix} \dot{x} + l\cos(\alpha)\dot{\alpha} + l_b\cos(\theta)\dot{\theta} \\ \dot{z} + l\sin(\alpha)\dot{\alpha} + l_b\sin(\theta)\dot{\theta} \end{bmatrix}, \ \dot{\mathbf{P}}_2 = \begin{bmatrix} \dot{x} + l\cos(\alpha)\dot{\alpha} + l_g\cos(\theta)\dot{\theta} \\ \dot{z} + l\sin(\alpha)\dot{\alpha} + l_g\sin(\theta)\dot{\theta} \end{bmatrix}. \tag{2.10}$$

We then obtain the Lagrangian

$$\begin{aligned} \mathcal{L} = &\frac{1}{2}m_0(\dot{z}^2 + \dot{x}^2) + \frac{1}{2}m_2(\dot{x} + l\cos(\alpha)\dot{\alpha} + l_g\cos(\theta)\dot{\theta})^2 \\ &+ (\dot{z} + l\sin(\alpha)\dot{\alpha} + l_g\sin(\theta)\dot{\theta})^2) + \frac{1}{2}J\dot{\theta}^2\rho \\ &+ V_t\rho g(z - l\cos(\alpha) - l_b\cos(\theta)) \\ &- m_2 g(z - l\cos(\alpha) - l_g\cos(\theta)). \end{aligned} \tag{2.11}$$

And now solving

$$\begin{aligned} \frac{d}{dt}(\frac{\partial \mathcal{L}}{\partial \dot{x}}) - \frac{\partial \mathcal{L}}{\partial x} = Q_x, \quad \frac{d}{dt}(\frac{\partial \mathcal{L}}{\partial \dot{z}}) - \frac{\partial \mathcal{L}}{\partial z} = Q_z, \\ \frac{d}{dt}(\frac{\partial \mathcal{L}}{\partial \dot{\alpha}}) - \frac{\partial \mathcal{L}}{\partial \alpha} = Q_\alpha, \quad \frac{d}{dt}(\frac{\partial \mathcal{L}}{\partial \dot{\theta}}) - \frac{\partial \mathcal{L}}{\partial \theta} = Q_\theta. \end{aligned} \tag{2.12}$$

We end up with a system on the form

$$\boldsymbol{D}(\boldsymbol{\gamma})\ddot{\boldsymbol{\gamma}} + \boldsymbol{C}(\boldsymbol{\gamma}, \dot{\boldsymbol{\gamma}})\dot{\boldsymbol{\gamma}} + \boldsymbol{G}(\boldsymbol{\gamma}) = \boldsymbol{Q}, \tag{2.13}$$

where

$$\begin{aligned} \boldsymbol{D} &= \begin{bmatrix} m_0 + m_2 & 0 & lm_2\cos(\alpha) & l_g m_2\cos(\theta) \\ 0 & m_0 + m_2 & lm_2\sin(\alpha) & l_g m_2\sin(\theta) \\ lm_2\cos(\alpha) & lm_2\sin(\alpha) & l^2 m_2 & ll_g m_2\cos(\alpha-\theta) \\ l_g m_2\cos(\theta) & l_g m_2\sin(\theta) & ll_g m_2\cos(\alpha-\theta) & J + l_g^2 m_2 \end{bmatrix} \\ \boldsymbol{C} &= \begin{bmatrix} 0 & 0 & -lm_2\sin(\alpha)\dot{\alpha} & -l_g m_2\sin(\theta)\dot{\theta} \\ 0 & 0 & lm_2\cos(\alpha)\dot{\alpha} & l_g m_2\cos(\theta)\dot{\theta} \\ 0 & 0 & 0 & ll_g m_2\sin(\alpha-\theta)\dot{\theta} \\ 0 & 0 & -ll_g m_2\sin(\alpha-\theta)\dot{\alpha} & 0 \end{bmatrix} \\ \boldsymbol{G} &= \begin{bmatrix} 0 \\ g((m_0+m_2) - V_r\rho) \\ gl(m_2 - \rho V_r)\sin(\alpha) \\ g(l_g m_2 - l_b V_r\rho)\sin(\theta) \end{bmatrix}. \end{aligned} \tag{2.14}$$

Generalized forces act on two points of the system: the buoy(P_0) and the CB(P_1) of the turbine. The generalized forces acting on P_0 are

$$Q_{x_{p0}} = \boldsymbol{F}\begin{bmatrix}1\\0\end{bmatrix}, \; Q_{y_{p0}} = \boldsymbol{F}\begin{bmatrix}0\\1\end{bmatrix}, \; Q_{\alpha_{p0}} = \boldsymbol{F}\begin{bmatrix}0\\0\end{bmatrix}, \; Q_{\theta_{p0}} = \boldsymbol{F}\begin{bmatrix}0\\0\end{bmatrix}, \tag{2.15}$$

and on P_1 are

$$Q_{x_{p1}} = \boldsymbol{F}\begin{bmatrix}1\\0\end{bmatrix}, \; Q_{y_{p1}} = \boldsymbol{F}\begin{bmatrix}0\\1\end{bmatrix}, \; Q_{\alpha_{p1}} = \boldsymbol{F}\begin{bmatrix}l\cos(\alpha)\\l\sin(\alpha)\end{bmatrix}, \; Q_{\theta_{p1}} = \boldsymbol{F}\begin{bmatrix}l_b\cos(\theta)\\l_b\sin(\theta)\end{bmatrix}, \tag{2.16}$$

or expressed as a matrix

$$\boldsymbol{Q}_{p_0} = \begin{bmatrix}1 & 0\\0 & 1\\0 & 0\\0 & 0\end{bmatrix}, \quad \boldsymbol{Q}_{p_1} = \begin{bmatrix}1 & 0\\0 & 1\\l\cos(\alpha) & l\sin(\alpha)\\l_b\cos(\theta) & l_b\sin(\theta)\end{bmatrix}. \tag{2.17}$$

2.3 Linear Wave Theory

When describing a wave, a few terms are commonly used in the literature [7]. The top of the wave is called the crest, and the lowest point is called the trough. The wavelength λ is the length from crest to crest. The wave amplitude ζ_a is the height from the still water line (SWL) to the crest, while the wave height H is the height from trough to crest.

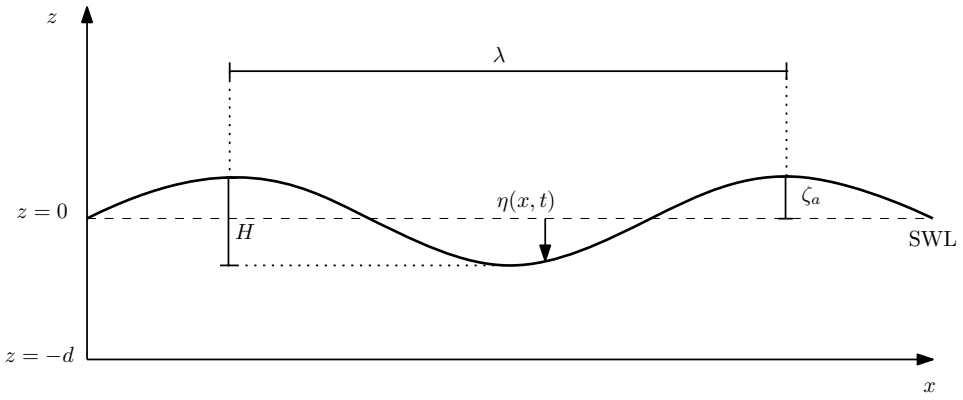

Figure 2.5: The buoy partially submerged in a wave, with submersion depth z_d, position z and wave-height z_w.

We also need a mathematical description of the motion of the waves in two dimensions. When describing waves, it's common to divide the waves into what depths of water we are working with, shallow waters, intermediate water, and deep water, and in this case, we would be at deep water, which is described as $d/\lambda > 0.5$ [8]. We assume that the waves are all traveling in the same direction. A description of the waves height $\eta(x,t)$, the waves velocity, and acceleration field are needed:

$$\eta(x,t) = \zeta_a \sin(\omega t - \kappa x) \tag{2.18}$$

$$u = \omega \zeta_a e^{\kappa z} \sin(\omega t - \kappa x) \tag{2.19}$$

$$w = \omega \zeta_a e^{\kappa z} \cos(\omega t - \kappa x) \tag{2.20}$$

$$\dot{u} = \omega^2 \zeta_a e^{\kappa z} \cos(\omega t - \kappa x) \tag{2.21}$$

$$\dot{w} = -\omega^2 \zeta_a e^{\kappa z} \sin(\omega t - \kappa x) \tag{2.22}$$

The horizontal velocity and acceleration are here u $\dot{u}$, while w and $\dot{w}$ are the vertical components. The wavenumber κ and angular frequency ω is related with

$$\omega = \sqrt{\kappa g}. \tag{2.23}$$

While the wavelength is related with

$$\lambda = \frac{2\pi}{\kappa}. \tag{2.24}$$

These equations give us the tools to describe the montion of a regular wave, a single wave with one frequency and wavelength. A simulation of the wave's velocity and acceleration field can be seen in figure 2.6.

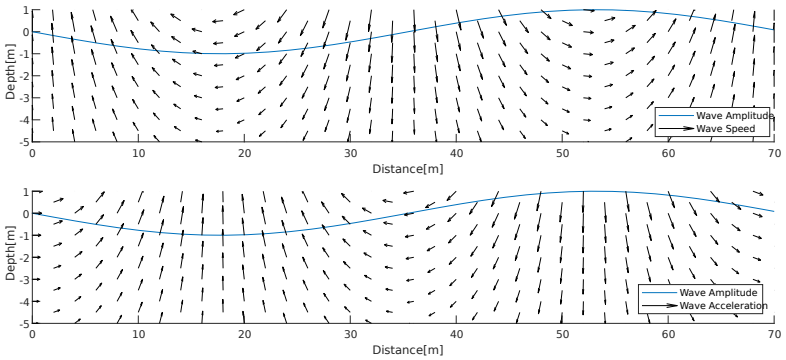

Figure 2.6: The wave's velocity is plotted on the top, with the accompanying wave elevation. On the bottom, the acceleration of the wave is plotted in the same fashion.

2.4 Ocean Waves

However, ocean waves are irregular waves, which means that they are a sum of many wave components, a sum of regular waves:

$$\eta(x,t) = \sum_{i=1}^{N} \zeta_i sin(\omega_i t - \kappa_i x + \epsilon_i) \tag{2.25}$$

ζ_i,ω_i, and κ_i are elements of the i-th wave, ϵ_i is the wave's random phase angle uniformly distributed between 0 and 2π, and is constant with time. The irregular waves' velocity and acceleration can be found in the same manner:

$$u = \sum_{i=1}^{N} u_i,\ w = \sum_{i=1}^{N} w_i,\ \dot{u} = \sum_{i=1}^{N} \dot{u}_i,\ \dot{w} = \sum_{i=1}^{N} \dot{u}_i \tag{2.26}$$

To describe a sea state a wave spectrum are used, these assume that the waves can be described as a stationary random process, and are called short term description of the sea because they are from a limited time window of 0.5 to 12 hours [7]. The amplitude of the wave component can be found from the wave spectrum with the relation

$$\zeta_i = \sqrt{2S(\omega_i)\Delta\omega}, \tag{2.27}$$

$S(\omega)$ is a wave spectrum, $\Delta\omega$ is a constant difference between frequencies.

A few different wave spectrums are developed. One of the most commonly used in the North sea is JONSWAP:

$$S(\omega) = 155\frac{H_s^2}{T_1^4}\omega^{-5}\exp(\frac{-944}{T_1^4}\omega^{-4})3.3^Y \tag{2.28}$$

$$Y = \exp\left[-(\frac{0.191\omega T_1 - 1}{\sqrt{2}\sigma})^2\right] \tag{2.29}$$

$$\sigma = \begin{cases} 0.07 & \text{for } \omega \leq 5.24/T_1 \\ 0.09 & \text{for } \omega > 5.24/T_1 \end{cases} \tag{2.30}$$

The significant wave height H_s is the mean height of 1/3 of the waves, while T_1 is the average wave period. Some other common wave spectrum descriptors are T_z, the average zero-crossing wave period, which is the inverse of the amount times the water level crosses the zero water level upward per second, and T_0 peak period. The relationship between them can be approximated as [9]:

$$T_1 = 1.073T_z \tag{2.31}$$

$$T_1 = 0.834T_0 \tag{2.32}$$

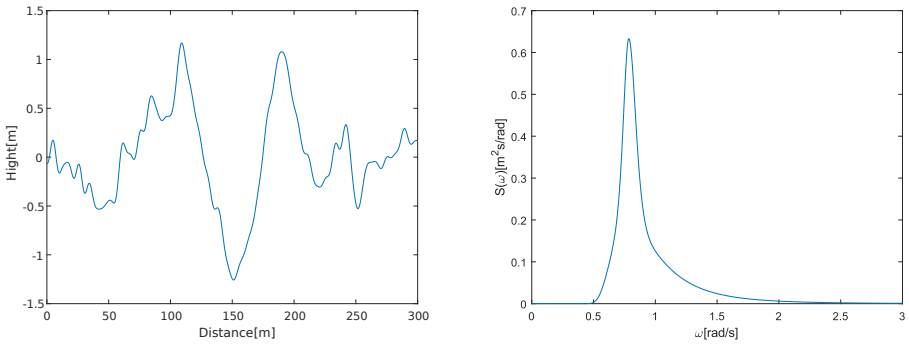

Figure 2.7: A wave simulated with the JONSWAP spectrum, where $H_s = 2$ and $T_z = 6.22$. To the right is the spectrum used for the wave.

2.5 Hydrostatics

Now, to calculate the buoyancy force of the buoy, the submerged volume of the buoy needs to be calculated. We assume that the water level is equal over the entire buoy, which then gives us the integral

$$\nabla_b = \int_{z-r}^{\eta} \pi(r^2 - (\hat{z} - z)^2)\, d\hat{z}. \tag{2.33}$$

The buoyancy force for the buoy is then

$$F_{b_b} = \rho g \nabla_b. \tag{2.34}$$

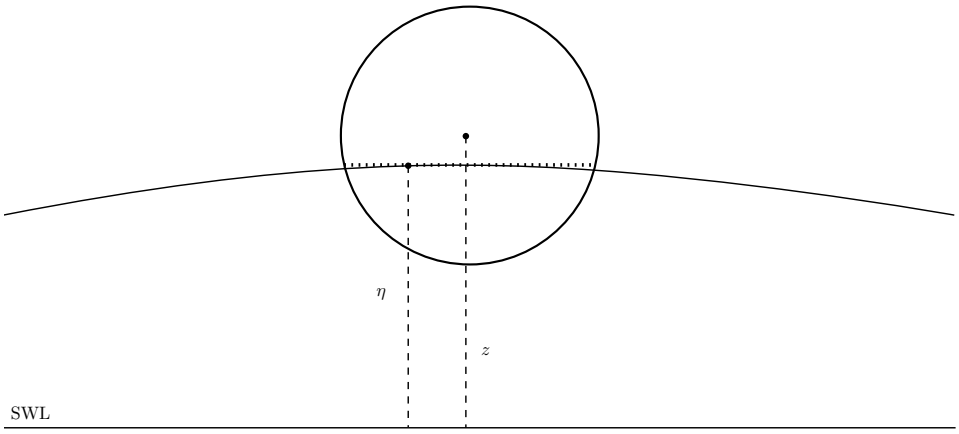

Figure 2.8: A visualization of the buoy sitting in a wave, with the even wave height drawn in.

2.6 Wave Forces

The turbine is submerged too deep to be affected by the wave forces, that is, over half a wavelength deep. However, the buoy is affected by wave forces. A model of these forces' interaction with the buoy is needed as this governs the speed of the turbine. And as follows the amount of lift generated by the control wings. In calculating hydrodynamic forces, the assumption is that the fluid is inviscid and irrotational. Bernoulli's equation is then used to integrate the pressure over the vessel's surface to get the hydrodynamic forces.
These processes are not discussed further here, but the software is used for calculating these forces is based on both 2D-strip theory and 3D-Potential theory.

However, to capture the dynamic motion, some other approach is needed, and there has been presented an approach that uses Morison equations to approximate the hydrodynamic forces on the buoy [10]. They have managed to get good results using Morison with strip theory to model the wave forces in heave and surge. Empirical data verified their simulations, allowing for a straightforward method to model the wave forces. Morison's equation is a semi-empirical equation that is used to calculate the hydrodynamic forces on slender objects, that is when $D/\lambda < 0.05$ [11].
Before introducing the equation, a quick introduction of the wave forces acting on an object.

If one picture an undisturbed wave-field, without any object in the water, as shown in figure 2.6. Then the wave's acceleration creates dynamic pressure on the submerged body that produces a force.
This force is named The Froude-Krylov force and is together diffraction force called the excitation force of the wave. In Morison, the wave acceleration field is assumed to be small varying over the body, so its set as a constant over the submerged body's horizontal direction.

Diffraction force is when the incoming wave-field hits the object sitting the waters and reflects/diffracts waves back that need to be taken into account as seen in figure 2.9. However, thin objects do not produce any significant diffraction (see fig 2.10), so the term is dropped in Morison's equation.

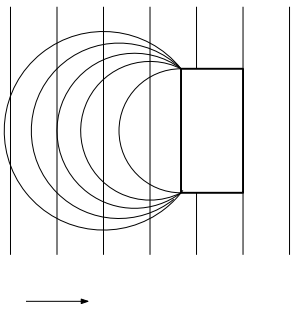

Figure 2.9: A bigger object in a wave-field causing diffraction

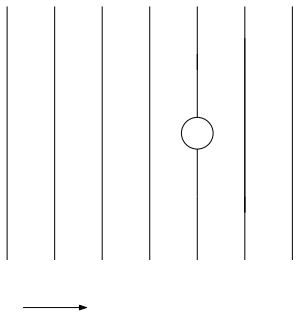

Figure 2.10: Slender object in wave-field

Now, if we look at an object in still waters accelerating under some force, that force would also need to move the surrounding water. That is, the object appears to have some added mass to it. For an object floating on the surface, this force is frequency dependent on the object's oscillations.
If one pictures a boat under control by some DP system, it oscillates back and forth around some given position. This movement creates some waves carrying energy away from the system. The water under the surface would also need to be moved as mentioned.

When calculated by the software in one of the mentioned methods, it gives $\mathbf{A}(\omega)$ and $\mathbf{B}(\omega)$ which are the added mass and dampening matrices, respectively, often referred to as the radiation force of the waves.
While the matrices over are given in the frequency domain, an equal equation in the time domain is

$$\boldsymbol{\tau}_{rad} = -\boldsymbol{A}(\infty) + \boldsymbol{\mu}_{rad}. \tag{2.35}$$

Where $\boldsymbol{A}(\infty)$ is the infinity added mass matrix. It can be thought of as the added mass that comes from the water not generating waves. While μ_{rad} is the energy lost due to waves being generated. In Morrison's equation, μ_{rad} is dropped, as again, due to the slender nature of the object, the waves generated can be neglected.

The last part is the drag force, and this is due to the viscous friction of the fluid. And are represented as the standard quadratic drag equation.

Now Morions equation [12] for an object in motion in a wave-field is then

$$dF = \rho A\dot{u} + \rho C_{a_b} A(\dot{u} - \ddot{x}) + \frac{1}{2}\rho C_{d_b} D(u - \dot{x})|u - \dot{x}|dz, \tag{2.36}$$

where dF is the force acting on a strip of length dz_s.

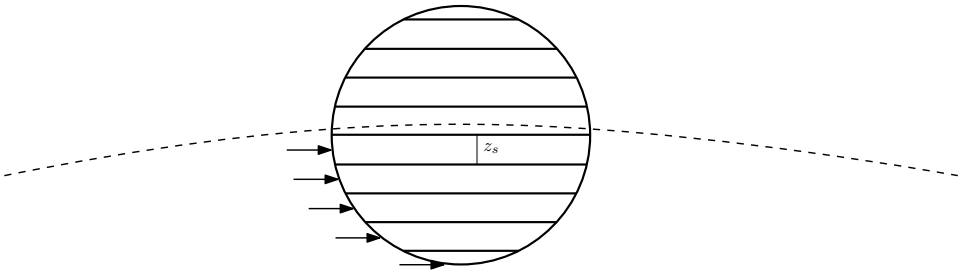

Figure 2.11: The buoy and wave forces acting on the strips z_s

The first part of the left side of the equation is the Froud-Krylov force, A is the area of the strip, and $\dot{u}$ is the wave velocity. This term depends on the wave velocity as it generates the dynamic pressure, independent of the velocity of the buoy.

The second term is then the added mass force, where C_{a_b} is the added mass coefficient. The coefficient is depended on the shape of the object. $\ddot{x}$ is the acceleration of the buoy. The added mass and Froud-Krylov force are often combined for a non-moving object into an inertial force term.

The last term is then the quadratic drag force. Where C_{d_b} is the drag coefficient, it usually depends on the Reynolds number and the object's shape but is often found empirical. D is then the diameter of the strip.

Then to get the total force acting on the buoy, integration over the submerged part of buoy is done.

$$F = \int_{z-r}^{\eta} \rho A\dot{u} + \rho C_{a_b} A(\dot{u} - \ddot{x}) + \frac{1}{2}\rho C_{d_b} D_h (u - \dot{x})|u - \dot{x}|\, dz. \tag{2.37}$$

Similarly, the heave wave forces can be expressed

$$F = \int_{z-r}^{\eta} \rho A\dot{u} + \rho C_{a_b} A(\dot{w} - \ddot{z}) + \frac{1}{2}\rho C_{d_b} D_v (w - \dot{z})|w - \dot{z}|\, dz. \tag{2.38}$$

2.7 Turbine Forces

As with the buoy, the turbine has an added mass component, and it is, according to [9] possible to consider this an added kinetic energy:

$$T_m = \frac{1}{2} m_{a_t} ||\dot{\boldsymbol{P}}_1||^2 \tag{2.39}$$

It is then added to the Lagrangian in (2.11) as a constant additional mass. This an approximation because the added mass is, in reality, a matrix of constants. The major way this would come into play, in a different added mass for x and z acceleration. However, the added mass for a cylinder is 1 [13], and when looking at the system from the top, the added mass from the turbine blades with the topside of the cylinder could be approximated as a circle that has the same added mass coefficient. Allowing for a lot cleaner equations of motion without too much loss of accuracy, especially since more precise coefficients are not available at this time.

The other main force acting on the turbine is drag force. At the operating depths of the turbine, we do still have ocean currents, and these are assumed slow time-varying, and irrotational. The current generates a drag force across the turbine to move it away from the desired position below the buoy. And we have the turbine movement itself in the heave, which depends on the wave state, in this direction, the drag force is the drag from the turbine body and turbine rotors. They would add a noticeable amount

of drag force.
We are, however, here interested in the best case for the control system, so the main drag from the turbine rotors are neglected.
An aspect that needs to be taken into account is that to generate a control force by the wings, the wings themselves have an area. That area will then again contribute to more drag, as illustrated in figure 2.12.
The drag force acting on the turbine is then

$$\frac{1}{2}\rho(C_{d_{t_x}}A_t + C_{d_w}2A_w)(u_c - \dot{P}_{1x})|u_c - \dot{P}_{1x}|, \tag{2.40}$$

a sum of the two drag forces as mention, where $\dot{P}_{1x}$ is the speed of CO in heave.
The amount of control force is the amount of lift generated by the wings, and this is expressed with the lift equation

$$F_l = \frac{1}{2}\rho A_w C_l(\alpha_w)\dot{P}_{1y}^{\,2}. \tag{2.41}$$

While the coefficient of lift C_l is a number deepening on factors like angle of attack and Reynolds number, it can be approximated with [14]

$$C_l(\alpha_w) \approx \frac{2\pi AR}{2 + AR}\alpha_w, \quad AR = \frac{s^2}{A_w}. \tag{2.42}$$

Where s is the span of the wings, and α_w is the angle of attack.

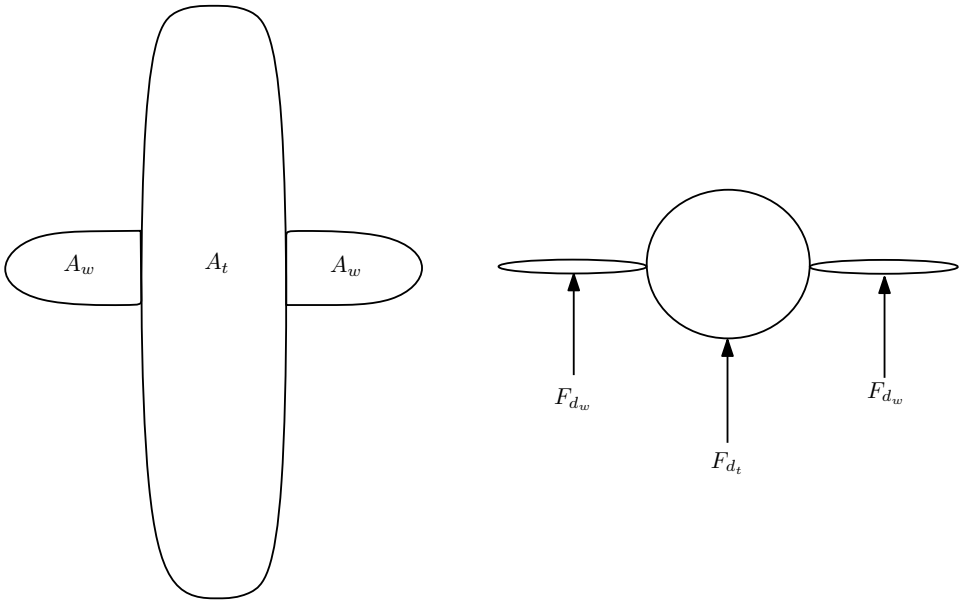

Figure 2.12: The projected area of the turbine with the control wings and the drag forces acting on the turbine.

2.8 Nonlinear Model

Now we want to combine the model (2.13) and the added mass from (2.39). We also separate the added mass from Morison that depend on the buoy acceleration

$$\boldsymbol{Q}_m = \begin{bmatrix} 1 & 0 \\ 0 & 1 \\ 0 & 0 \\ 0 & 0 \end{bmatrix} \begin{bmatrix} \int_{z-r}^{\eta} \rho A\dot{u} + \rho C_{a_b} A(\dot{u} - \ddot{x}) + \frac{1}{2}\rho C_{d_b} D_h (u - \dot{x})|u - \dot{x}|\, dz \\ \int_{z-r}^{\eta} \rho A\dot{w} + \rho C_{a_b} A(\dot{w} - \ddot{z}) + \frac{1}{2}\rho C_{d_b} D_v (w - \dot{z})|w - \dot{z}|\, dz \end{bmatrix}, \tag{2.43}$$

$$\boldsymbol{Q}_m = \begin{bmatrix} \int_{z-r}^{\eta} \rho A\dot{u} + \rho C_{a_b} A\dot{u} + \frac{1}{2}\rho C_{d_b} D_h (u - \dot{x})|u - \dot{x}|\, dz \\ \int_{z-r}^{\eta} \rho A\dot{w} + \rho C_{a_b} A\dot{w} + \frac{1}{2}\rho C_{d_b} D_v (w - \dot{z})|w - \dot{z}|\, dz \\ 0 \\ 0 \end{bmatrix}. \tag{2.44}$$

This gives new **G** and **C** matrices.

$$\begin{aligned} \boldsymbol{D} &= \begin{bmatrix} m_b + m_t & 0 & lm_t\cos(\alpha) & l_g m_t \cos(\theta) \\ 0 & m_b + m_t & lm_t \sin(\alpha) & l_g m_t \sin(\theta) \\ lm_t\cos(\alpha) & lm_t \sin(\alpha) & l^2 m_t & ll_g m_t \cos(\alpha - \theta) \\ l_g m_t \cos(\theta) & l_g m_t \sin(\theta) & ll_g m_t cos(\alpha - \theta) & J + l_g^2 m_t \end{bmatrix}, \\ \boldsymbol{C} &= \begin{bmatrix} 0 & 0 & -lm_t \sin(\alpha)\dot{\alpha} & -l_g m_t \sin(\theta)\dot{\theta} \\ 0 & 0 & lm_t \cos(\alpha)\dot{\alpha} & l_g m_t \cos(\theta)\dot{\theta} \\ 0 & 0 & 0 & ll_g m_t \sin(\alpha - \theta)\dot{\theta} \\ 0 & 0 & -ll_g m_t \sin(\alpha - \theta)\dot{\alpha} & 0 \end{bmatrix}. \end{aligned} \tag{2.45}$$

Where

$$m_b = m_0 + \rho C_{a_b} V_b(t), \quad m_t = m_2 + \rho C_{a_t} V_t. \tag{2.46}$$

The stiffness matrix **G** is not affected in any way since it only depends on mass and volume.

Now the rest of the forces acting on the turbine is going to be expressed as

$$\boldsymbol{Q}_d = \begin{bmatrix} 1 & 0 \\ 0 & 1 \\ l\cos(\alpha) & l\sin(\theta) \\ lb\cos(\alpha) & lb\sin(\theta) \end{bmatrix} \begin{bmatrix} -\frac{1}{2}\rho(C_{d_{t_x}} A_t + C_{d_w} 2A_w)(v_c - \dot{P}_{1x})|v_c - \dot{P}_{1x}| \\ -\frac{1}{2}\rho C_{d_{t_z}} \dot{P}_{1y}|\dot{P}_{1y}| \end{bmatrix}, \tag{2.47}$$

$$\boldsymbol{Q}_d = \begin{bmatrix} -\frac{1}{2}\rho(C_{d_{t_x}} A_t + C_{d_w} 2A_w)(v_c - \dot{P}_{1x})|v_c - \dot{P}_{1x}| \\ -\frac{1}{2}\rho C_{d_{t_z}} \dot{P}_{1y}|\dot{P}_{1y}| \\ -\frac{1}{2}\rho(C_{d_{t_x}} A_t + C_{d_w} 2A_w)(v_c - \dot{P}_{1x})|v_c - \dot{P}_{1x}| l\cos(\alpha) - \frac{1}{2}\rho C_{d_{t_z}} \dot{P}_{1y}|\dot{P}_{1y}| l\sin(\alpha) \\ -\frac{1}{2}\rho(C_{d_{t_x}} A_t + C_{d_w} 2A_w)(v_c - \dot{P}_{1x})|v_c - \dot{P}_{1x}| l_b\cos(\theta) - \frac{1}{2}\rho C_{d_{t_z}} \dot{P}_{1y}|\dot{P}_{1y}| l_b\sin(\theta) \end{bmatrix}, \tag{2.48}$$

where v_c is the current velocity. The lift force is

$$\boldsymbol{Q}_l = \begin{bmatrix} 1 & 0 \\ 0 & 1 \\ l\cos(\alpha) & l\sin(\theta) \\ lb\cos(\alpha) & lb\sin(\theta) \end{bmatrix} \begin{bmatrix} \frac{1}{2}\rho A_w C_l \dot{P}_{1y}^{\,2} \alpha_w \\ 0 \end{bmatrix}, \tag{2.49}$$

$$\boldsymbol{Q}_l = \begin{bmatrix} \frac{1}{2}\rho A_w C_{l_\alpha} \dot{P}_{1y}^{\,2} \alpha_w \\ 0 \\ l cos(\alpha)\frac{1}{2}\rho A_w C_l \dot{P}_{1y}^{\,2} \alpha_w \\ l_b cos(\alpha)\frac{1}{2}\rho A_w C_l \dot{P}_{1y}^{\,2} \alpha_w \end{bmatrix}. \tag{2.50}$$

Lastly, adding in the buoyancy acting on the as

$$\boldsymbol{G} = \begin{bmatrix} 0 \\ g((m_0 + m_2) - (V_r + V_b(t))\rho) \\ gl(m_2 - \rho V_r)\sin(\alpha) \\ g(l_g m_2 - l_b V_r \rho)\sin(\theta) \end{bmatrix}. \tag{2.51}$$

Giving a complete system with (2.45)(2.44)(2.48)(2.50)(2.51) as

$$\boldsymbol{D}(\boldsymbol{\gamma})\ddot{\boldsymbol{\gamma}} + \boldsymbol{C}(\boldsymbol{\gamma}, \dot{\boldsymbol{\gamma}})\dot{\boldsymbol{\gamma}} + \boldsymbol{G}(\boldsymbol{\gamma}) = \boldsymbol{Q}_m + \boldsymbol{Q}_d + \boldsymbol{Q}_l. \tag{2.52}$$

Giving a solid mathematical model as a basis for further analyses of the system.

Chapter 3

Linearization and Control

In this section, a linear model is derived from the nonlinear one to develop a controller for the system.

3.1 Small Angle Approximation and Linearization

Now to derive a linear model, the first step is to assume small angles. This assumption is safe to make, as the turbine won't drift that far off-center compared to the length of the rope. Nor will it tilt far from 0 degrees due to the restoring moment from the ballast. For reference, small-angle approximation says that

$$\sin(x) \approx x, \quad \cos(x) \approx 1. \tag{3.1}$$

Applying (3.1) on (2.13), we get the new system

$$\begin{bmatrix} m_b+m_t & 0 & lm_t & l_g m_t \\ 0 & m_b+m_t & lm_t\alpha & l_g m_t\theta \\ lm_t & lm_t\alpha & l^2 m_t & ll_g m_t(\alpha\theta+1) \\ l_g m_t & l_g m_t\theta & ll_g m_t(\alpha\theta+1) & J+l_g^2 m_t \end{bmatrix} \ddot{\gamma} + \begin{bmatrix} 0 & 0 & -lm_t\alpha\dot{\alpha} & -l_g m_t\theta\dot{\theta} \\ 0 & 0 & lm_t\dot{\alpha} & l_g m_t\dot{\theta} \\ 0 & 0 & 0 & ll_g m_t(\alpha-\theta)\dot{\theta} \\ 0 & 0 & -ll_g m_t(\alpha-\theta)\dot{\alpha} & 0 \end{bmatrix} \dot{\gamma} + \begin{bmatrix} 0 \\ g((m_0+m_2)-V_r\rho) \\ gl(m_2-\rho V_r)\alpha \\ g(l_g m_2 - l_b V_r\rho)\theta \end{bmatrix} = \boldsymbol{Q}. \tag{3.2}$$

We also view $\boldsymbol{Q}$ as

$$\boldsymbol{Q} = \boldsymbol{Q}_l + \boldsymbol{d}, \tag{3.3}$$

because we view the other external forces as disturbances acting on the linear system. $\boldsymbol{Q}_l$ with a small-angle approximation is

$$\boldsymbol{Q}_l = \begin{bmatrix} F_l \\ 0 \\ F_l l \\ F_l l_b \end{bmatrix}. \tag{3.4}$$

Further, we assume low speeds, and this makes the entire Coriolis matrix fall away, such that

$$\dot{\boldsymbol{\gamma}}^2 \approx \boldsymbol{0}. \tag{3.5}$$

We also assume neutral buoyancy, and as a result, constant submerged volume and added mass for the buoy

$$g((m_0 + m_2) - V_r\rho - V_b\rho) = 0, \tag{3.6}$$

$$m_b = m_0 + \rho C_{a_b} V_{b_k}, \tag{3.7}$$

leaving us with the system

$$\begin{bmatrix} m_0+m_2 & 0 & lm_2 & l_g m_2 \\ 0 & m_0+m_2 & lm_2\alpha & l_g m_2\theta \\ lm_2 & lm_2\alpha & l^2 m_2 & ll_g m_2(\alpha\theta+1) \\ l_g m_2 & l_g m_2\theta & ll_g m_2(\alpha\theta+1) & J + l_g^2 m_2 \end{bmatrix} \ddot{\boldsymbol{\gamma}} + \begin{bmatrix} 0 \\ 0 \\ gl(m_2 - \rho V_r)\alpha \\ g(l_g m_2 - l_b V_r \rho)\theta \end{bmatrix} = \boldsymbol{Q}. \tag{3.8}$$

We separate the acceleration terms for the system,

$$\ddot{\boldsymbol{\gamma}} = \boldsymbol{D}(\boldsymbol{\gamma})^{-1}(\boldsymbol{Q}_l - \boldsymbol{G}(\boldsymbol{\gamma})). \tag{3.9}$$

Since we are interested in controlling the angle and not the angular speed, we need to separate the system into two linear differential equations. We also linearise around the working position and force

$$\boldsymbol{\gamma}, F_l \to 0. \tag{3.10}$$

That gives us the linear system

$$\dot{\varsigma} = \boldsymbol{A}\varsigma + \boldsymbol{B}u, \tag{3.11}$$

$$\boldsymbol{A} = \begin{bmatrix} \mathbf{0} & I \\ \boldsymbol{D}(0)^{-1}\dfrac{d\boldsymbol{G}(0)}{d\gamma} & \mathbf{0} \end{bmatrix}, \quad \boldsymbol{B} = \begin{bmatrix} \mathbf{0} \\ \boldsymbol{D}(0)^{-1}Q_l \end{bmatrix}. \tag{3.12}$$

Or in its complete form

$$\boldsymbol{A} = \begin{bmatrix} 0 & 0 & 0 & 0 & 1 & 0 & 0 & 0 \\ 0 & 0 & 0 & 0 & 0 & 1 & 0 & 0 \\ 0 & 0 & 0 & 0 & 0 & 0 & 1 & 0 \\ 0 & 0 & 0 & 0 & 0 & 0 & 0 & 1 \\ 0 & 0 & \dfrac{g(m_2 - V_r)\rho}{m_b} & 0 & 0 & 0 & 0 & 0 \\ 0 & 0 & 0 & 0 & 0 & 0 & 0 & 0 \\ 0 & 0 & -\dfrac{g(l_g^2 m_b m_t + J(m_b + m_t))(m_2 - l_b V_r \rho)}{Jlm_b m_t} & \dfrac{gl_g(l_g m_2 - l_b V_r \rho)}{Jl} & 0 & 0 & 0 & 0 \\ 0 & 0 & \dfrac{gl_g(m_2 - V_r \rho)}{J} & \dfrac{g(l_b V_r \rho - l_g m_2)}{J} & 0 & 0 & 0 & 0 \end{bmatrix}$$

$$\boldsymbol{B} = \begin{bmatrix} 0 \\ 0 \\ 0 \\ 0 \\ 0 \\ 0 \\ \dfrac{J + l_g m_t(l_g - l_b)}{Jlm_t} \\ \dfrac{l_b - l_b}{J} \end{bmatrix}. \tag{3.13}$$

We can now use the linear system derived here to tune and implement a controller for the system, then use the controller for the non-linear system as shown in 3.1.

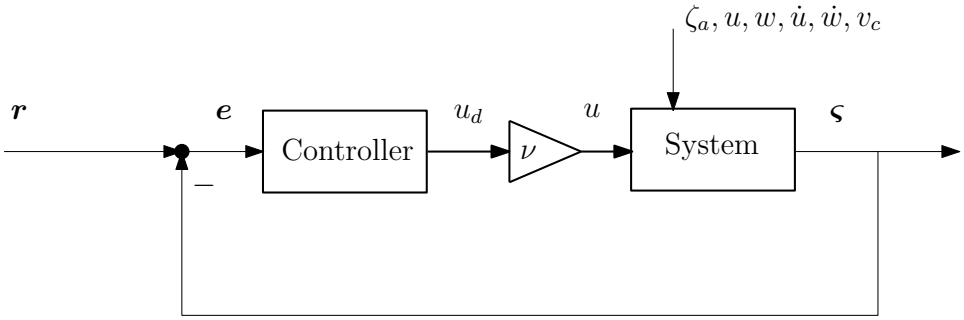

Figure 3.1: The system shown in the context of a feedback loop.

$\boldsymbol{r}$ is a vector of the system's set points, and in the case of this system, it would simply be zeros. The error term $\boldsymbol{e}$ is the difference between the setpoint, and the system states $\boldsymbol{\varsigma}$. u_d is the desired control from the controller. The constant λ is here as a scaling factor on the desired control signal, in the case of this model, that is, a single input, ν is the difference of the desired control force by the controller and what lift force the wings could produce u. Because the wings would be constrained to

$$-10^\circ < \alpha_w < 10^\circ, \tag{3.14}$$

to preserve laminar flow over them. In this case, this could be found by solving the lift equation within the set constraint. If control in yaw were to be added, this could be done by solving the force distribution as a QP problem. How this could be done was explored in the pre-project.

3.2 The Linear Quadratic Regulator

When choosing a multi-variable system controller, the ease of tuning and performance is essential. The LQR controller was found to give both good preference and intuitive tuning. LQR seeks to minimize the function [15]

$$J = \int_0^\infty \boldsymbol{x}^\intercal \mathbf{Q} \boldsymbol{x} + \boldsymbol{u}^\intercal \mathbf{R} \boldsymbol{u} \, dt. \tag{3.15}$$

Where $\mathbf{Q}$ and $\mathbf{R}$ and positive definite and symmetric weighting matrices, chosen as a tuning parameter of the controller.

The feedback law for the controller is

$$u_d = -\boldsymbol{K}\boldsymbol{\varsigma}, \qquad \boldsymbol{K} = \boldsymbol{R}^{-1}(\boldsymbol{B}^T\boldsymbol{P}). \tag{3.16}$$

The closed loop-system is then

$$\dot{\boldsymbol{\varsigma}} = (\boldsymbol{A} - \boldsymbol{B}\boldsymbol{R}^{-1}(\boldsymbol{B}^T\boldsymbol{P}))\boldsymbol{\varsigma}. \tag{3.17}$$

Where P is the symmetric solution to the algebraic Riccati equation

$$\mathbf{A}^\intercal\mathbf{P} + \mathbf{P}\mathbf{A} + \mathbf{Q} - (\mathbf{P}\mathbf{B})\mathbf{R}^{-1}(\mathbf{B}^\intercal\mathbf{P}) = \mathbf{0}. \tag{3.18}$$

If the matrix in (3.16) is Hurwitz, that is, the poles have negative real part. The feedback minimizes the LQR criterion (3.15).

Chapter 4

Simulation

In this section, the simulation results from the different aspects of the model are presented.

4.1 System Parameters

Buoy Parameters		
m_0	2200 Kg	Mass of Buoy
C_{a_b}	0.5	Added Mass Coefficient for Buoy
r_b	1.25 m	Raidus of Buoy
C_{d_b}	0.47	Drag Coefficient for Buoy
l	100 m	Rope Length
Turbine Parameters		
m_2	1500 Kg	Mass of Turbine
C_{a_t}	1	Added Mass Coefficient for Turbine
h_t	6 m	Hight of Turbine
d_t	0.4 m	Width of Turbine
l_g	5 m	Length from Top of Turbine to CG
l_b	3 m	Length from Top of Turbine to CB
V_t	0.754 m^3	Turbine Displacement
$C_{d_{t_x}}$	0.7	Turbine Body Drag Coefficient in x
$C_{d_{t_z}}$	1	Turbine Body Drag Coefficient in z
C_{d_w}	1.16	Turbine Wings Drag Coefficient in x
C_l	4.65	Coefficient of lift
Environmental Parameters		
g	9.81 m/s^2	Acceleration of Gravity
ρ	1024 kg/m^3	Sea Water Density

The accurate parameters for the system are hard to estimate without proper CAD models and software to calculate such numbers, or empirical data gathered, however with a few basic assumptions made and data provided by Waveco, reasonable parameters can be found.

The weight and buoyancy are taken as reference values from Automar product description. So for the buoy, the radius is taken so that a given buoyancy is met. The added mass for a sphere is then used, the same with the drag coefficient. The shape of the turbine body is approximated as a cylinder with a rounded nose. The parameters were chosen to be as close to design specifications as possible. The center of mass is moved down in the body to simulate the effect of the ballast. Appropriate parameters are then found in DNV - Modelling and Analysis of Marine Operations [13].

4.2 Implementation

The nonlinear model derived is implemented in Matlab and solved using the ode45 solver, with the different forces implemented as functions. A simulation window was made better to get an intuitive feeling for the system's dynamics, as shown in the figure under.

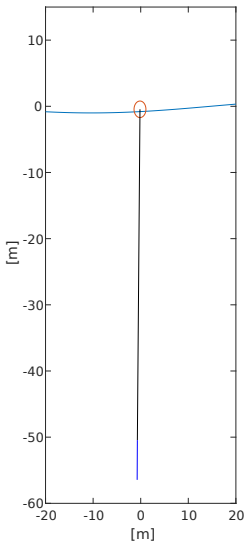

Figure 4.1: The system is visualized in Matlab, where the buoy can be seen in red, with the black rope connecting to the dark blue turbine at the bottom

4.3 Hydrodynamic Effects On The Buoy

We start by evaluating the free-floating buoy's hydrodynamic model to see if it performs as expected. To find an appropriate sea state, we can look to DNV - Wave loads [16].

We start by looking at the buoy's position in surge as shown in figure 4.2, where the plot shows the x position for the buoy under the effect of two different seized regular waves. Here we can observe the effects of Stokes drift, and its scaling up with the taller waves. It is a good indication that our model performs as desired.

Looking at the heave forces in figure 4.3, we can see that the wave load forces mainly depend on inertia force, that is, the Froude-Krylov and added mass force. These forces depend on the acceleration of the wave, and as can be seen, follow the wave's acceleration profile. The drag term is mostly small, except when the buoy hits the trough and breaks from the again rising waters. Oscillations can be observed in the total force, stemming from the buoyancy force.

In surge, we see the same behavior, with drag forces being player a more significant role as one would expect, with more water movement across the sides of the buoy. We can see that the buoy's speed is slightly higher on the wave crests, adding up to a slow movement with the waves due to the slightly higher vertical wave velocity in the wave crests than the trough.

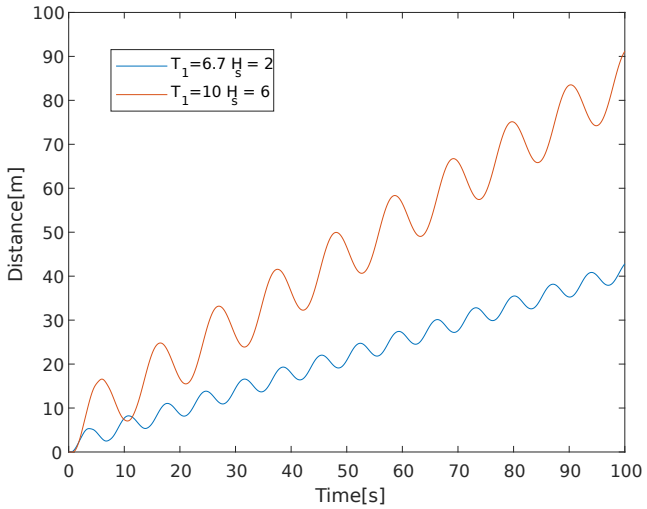

Figure 4.2: The buoys x-position plotted for two different wave sizes, showing the effects of stokes drift.

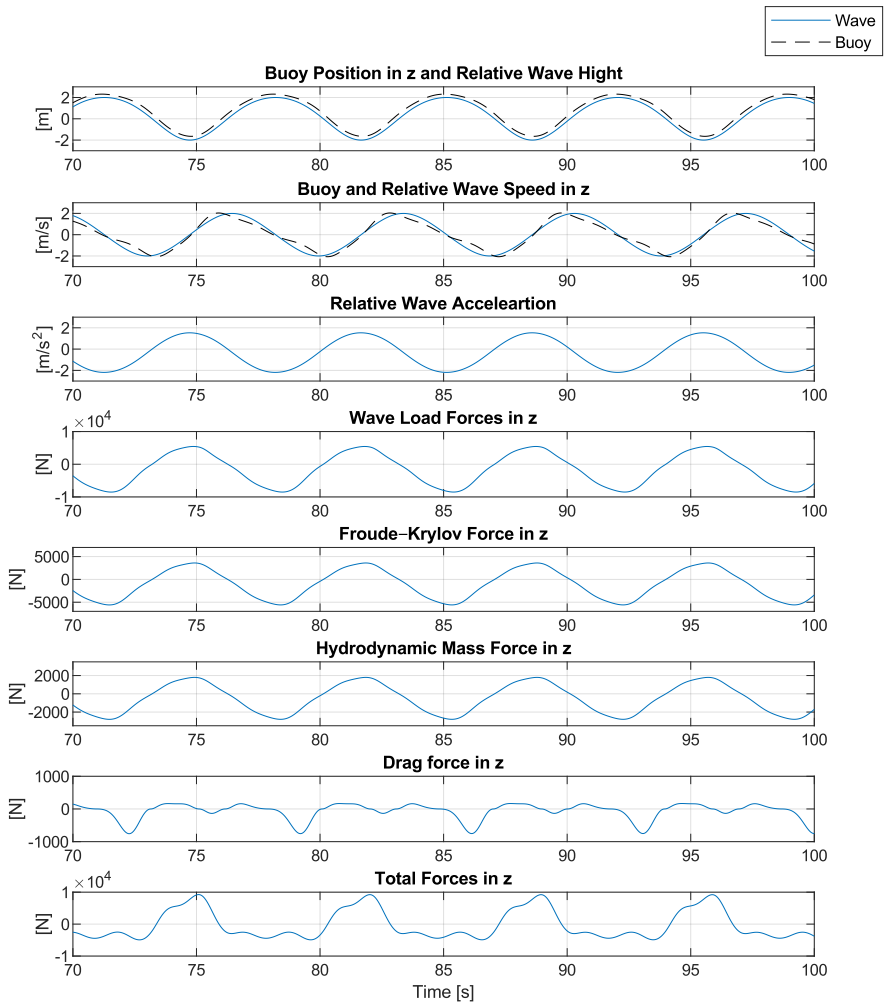

Figure 4.3: The wave forces acting on the buoy in heave, for a wave with $H = 2$ and $T_z = 8$.

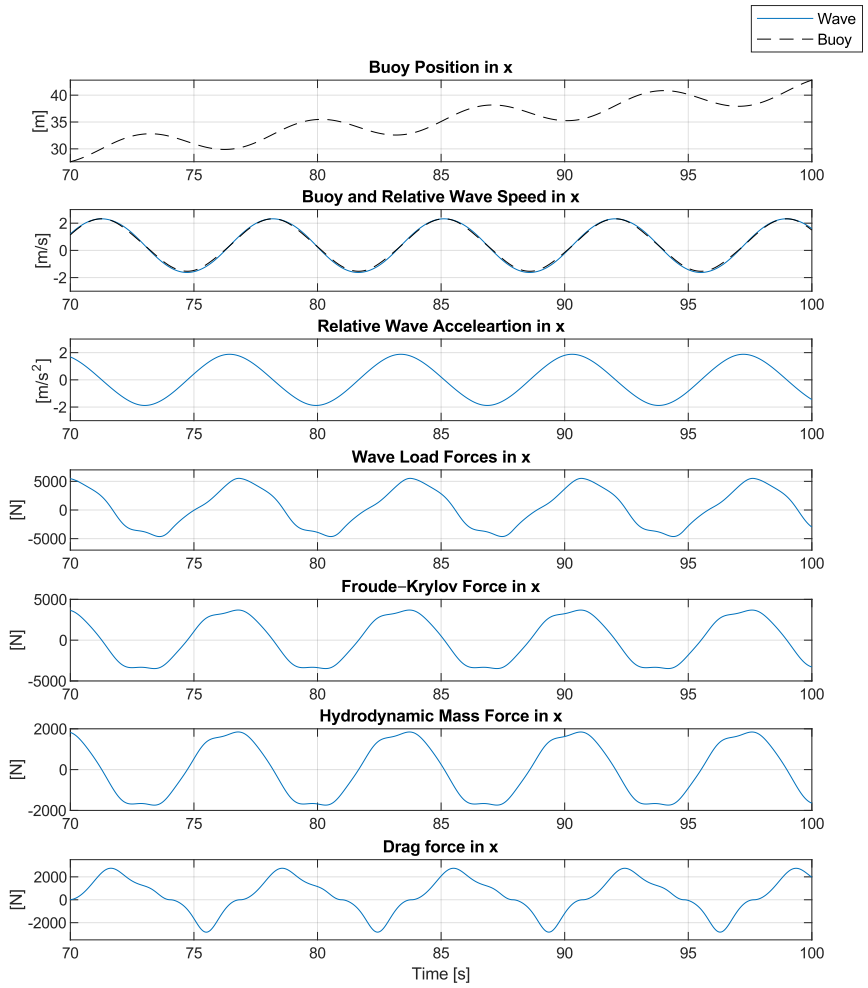

Figure 4.4: The wave forces acting on the buoy in surge, for a wave with $H = 2$ and $T_z = 8$.

The simulations seem to validate that the method presented by [10]holds up for an approximation of the wave load forces, giving us a good fundament for further analysis.

4.4 Nonlinear Model

When looking at the complete model, we still observe the wave-drift and see how the oscillating motion propagates down in the system as it gets carried away with the waves. While α follows the wave-drift oscillations almost perfectly, it can be seen that θ, while following the main motions, has a more complicated motion, in line with the more chaotic nature of a pendulum. The more interesting result is that we are talking about tiny numbers under likely wave conditions. While the motion affects the entire system, the displacement in the horizontal position from the buoy to the turbine is maximum 2 meters. Even when adding an ocean current of -0.3 m/s, we see little change in this behavior. However, the drag on the turbine does overcome the wave drift and drags the system in the current direction.

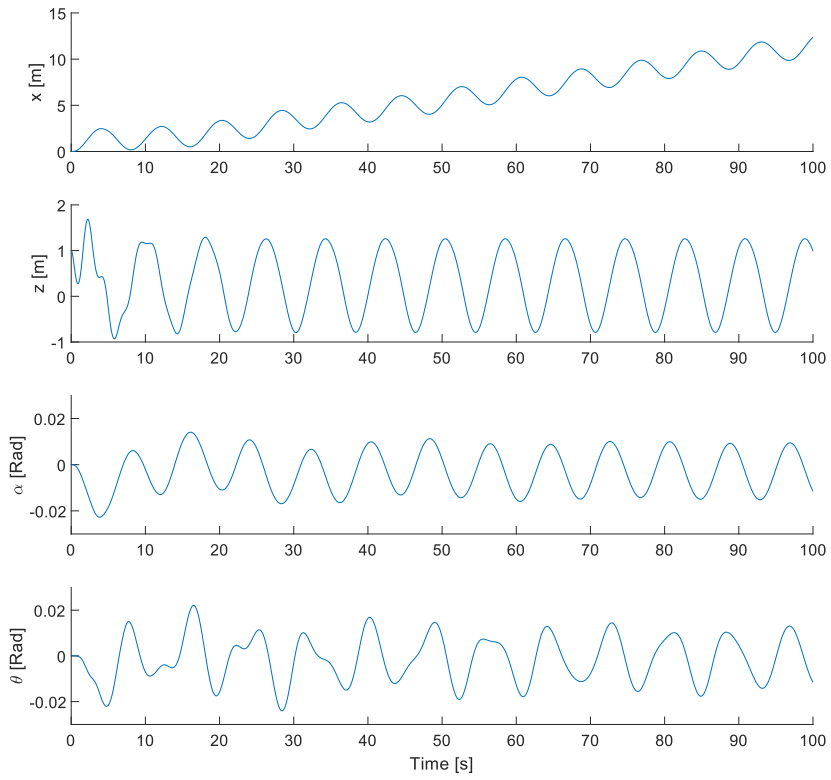

Figure 4.5: The full model with no current and a regular wave with $H = 2$ and $T_z = 7.45$.

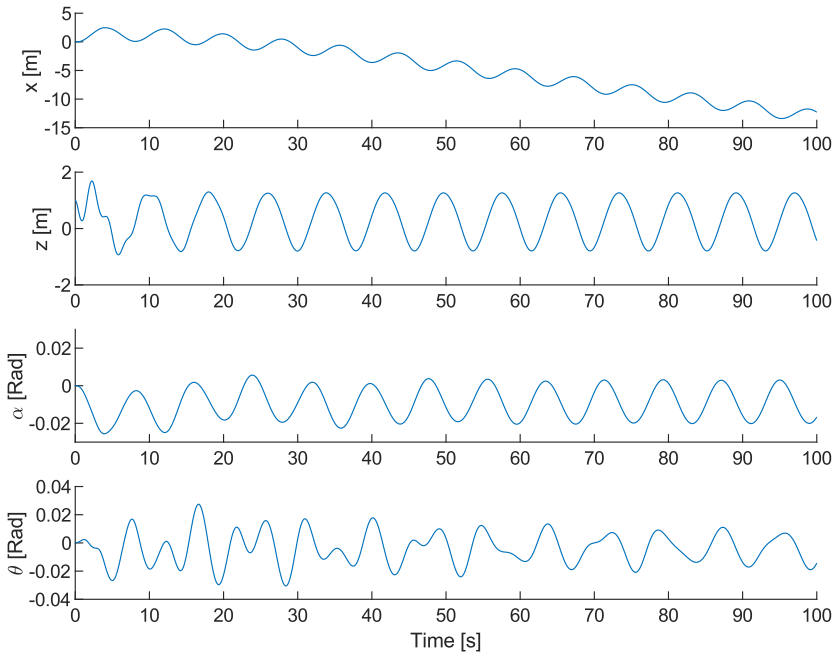

Figure 4.6: FThe full model with a current of -0.3 m/s and a regular wave with $H = 2$ and $T_z = 7.45$.

4.5 Performance for Linear Model

When using the provided parameters, we end up with a linear system with the matrices

$$\mathbf{A} = \begin{bmatrix} 0 & 0 & 0 & 0 & 1 & 0 & 0 & 0 \\ 0 & 0 & 0 & 0 & 0 & 1 & 0 & 0 \\ 0 & 0 & 0 & 0 & 0 & 0 & 1 & 0 \\ 0 & 0 & 0 & 0 & 0 & 0 & 0 & 1 \\ 0 & 0 & 2.98165 & 0 & 0 & 0 & 0 & 0 \\ 0 & 0 & 0 & 0 & 0 & 0 & 0 & 0 \\ 0 & 0 & -0.169573 & 0.127739 & 0 & 0 & 0 & 0 \\ 0 & 0 & 1.81931 & -2.55477 & 0 & 0 & 0 & 0 \end{bmatrix}, \mathbf{B} = \begin{bmatrix} 0 \\ 0 \\ 0 \\ 0 \\ 0 \\ 0 \\ 0.00000794 \\ -0.0000678 \end{bmatrix}. \quad (4.1)$$

In figure 4.7 we first see a direct comparison between the two models. However, the drag forces are removed from the non-linear model as they are not represented in the linear one. The result is an acceptable approximation for tuning the LQR Controller. We can observe that the differences are highest where expected, as with α when crossing zero degrees, and this is where the speed is highest and, as a result, where the linear model is least accurate.

There is, of course, some model deviations as time goes on, and this becomes apparent in θ, and might be partly due to the heavy motion in the non-linear model.

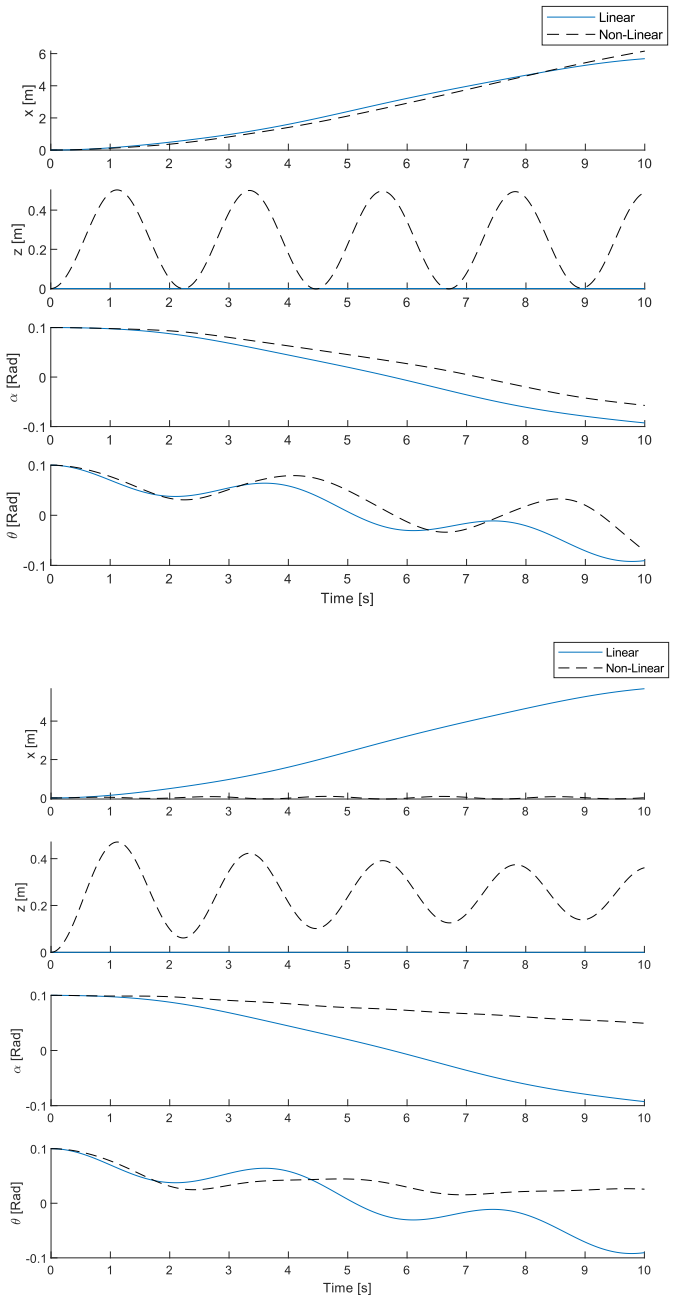

Figure 4.7: The linear and non-linear model, without drag-forces affecting either(Top) and drag forces affecting the non-linear system(Bottom).

However, as seen when the drag terms are included, the differences become more dramatic. The non-linear model is, of course, more damped, and the deviations grow fast. Nevertheless, we do expect the LQR controller to be robust so that it can handle the difference.

When wanting to extract force from the wings to control the system, the size and shape matter, as there is drag created by them and the turbine's body. And this has to be weighed against the amount of lift generated as discussed. In figure 4.8 a few different wing configurations are plotted against the drag force they create, with the greatest allowed angle of attack. The average turbine speed generated by a wave with $H = 1.5$ and $T_1 = 6.7$ is approximately 0.5 m/s. This is used as a low basis for the lift force generated, and a current of 0.3 m/s is used as a basis for the drag created. The different C_l is the constant part of (2.42), where longer spans create more lift, so by the same equation, if the area of the wing grows, do the span to keep the coefficient high. While only an estimate, moving forward wings with a span of 2 m each and a total area of 1.4 m^2 is used.

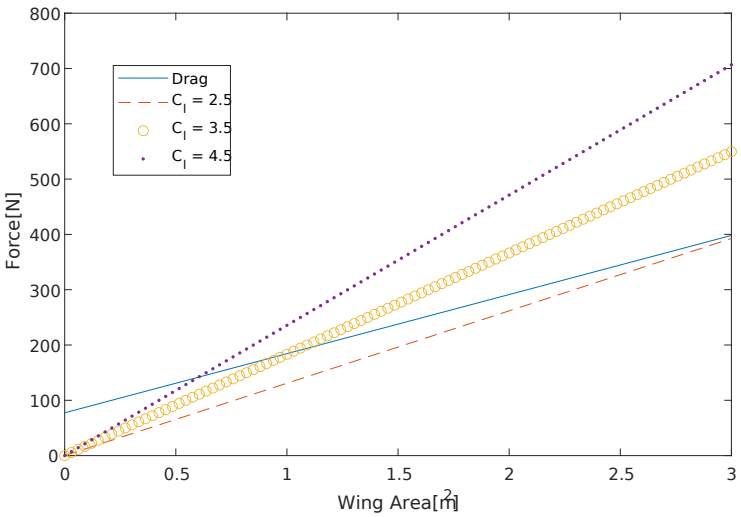

Figure 4.8: Drag forces of the wings with a fixed area, compared to the lift of the wings in different span configurations.

Now when closing the loop and attaching the LQR Controller, we start by first looking at the premise of the work done in the pre-project, that is, can such a system be used to position the system with the help of wave-forces. And as we can be seen from figure 4.9 this is achieved. The figure shows the system overcoming the wave load forces and a low ocean current of 0.2 m/s.

This while also keeping a low angle on both α and θ. The horizontal displacement of the turbine relative to the buoy would be at most a few meters—however, we why this might have issues on its own later.

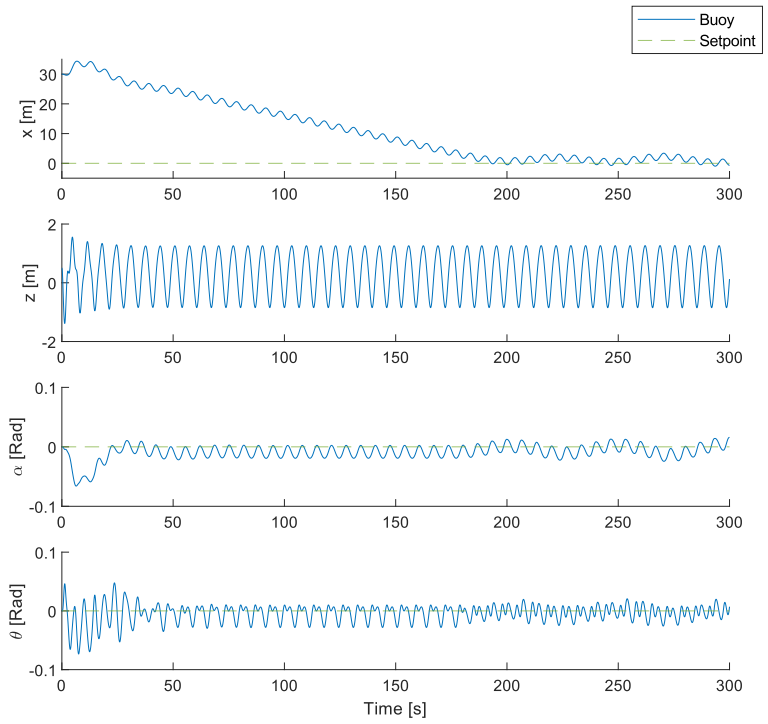

Figure 4.9: The turbine could be used to move the buoy under the influence of wave forces and ocean currents acting on the turbine, simulated with a regular wave with $H = 2$ and $T_1 = 5.6$.

The premise of the system as presented by Waveco is that the buoy itself is tethered to some anchoring system as mentioned or kept in place by a DP system when used as an observation buoy. So moving forward, we assume that it is kept in place, and we make a simple model for this by spring locking the system in x-direction. We update our model by adding

$$F_s = kx. \tag{4.2}$$

And the new $\mathbf{A}$ in the linear model becomes

$$\mathbf{A} = \begin{bmatrix} 0 & 0 & 0 & 0 & 1 & 0 & 0 & 0 \\ 0 & 0 & 0 & 0 & 0 & 1 & 0 & 0 \\ 0 & 0 & 0 & 0 & 0 & 0 & 1 & 0 \\ 0 & 0 & 0 & 0 & 0 & 0 & 0 & 1 \\ -11.11 & 0 & 2.98165 & 0 & 0 & 0 & 0 & 0 \\ 0 & 0 & 0 & 0 & 0 & 0 & 0 & 0 \\ 0.1111 & 0 & -0.169573 & 0.127739 & 0 & 0 & 0 & 0 \\ 0 & 0 & 1.81931 & -2.55477 & 0 & 0 & 0 & 0 \end{bmatrix}. \tag{4.3}$$

When looking at the system locked in place in figure 4.10 a few things become apparent. First and formost is that under these conditions that is a ocean current of 0.3 m/s, there is little to gain on having control wings. While the controller manges the keep the turbine in place under the buoy, the displacement without the controll system is minor to begin with. Also, adding more movement in θ, while not by a lot, is a downside.

Now what can be perhaps seen as a worst-case for the control system is shown in 4.11, where a stronger current is pulling on the system in combination with relatively low waves. There is not enough lift force generated to make up for the added drags of the wings. While a current of that strength is uncommon, at least in the Norwegian Sea, it highlights a weakness of the approach.

Showing the same scenario again in figure 4.12 with higher wave amplitude, we see that we again gain performance, but at the cost of higher oscillations in θ. The wings are mounted higher than the center of gravity, so this can not be avoided when pulling more force from the wings.

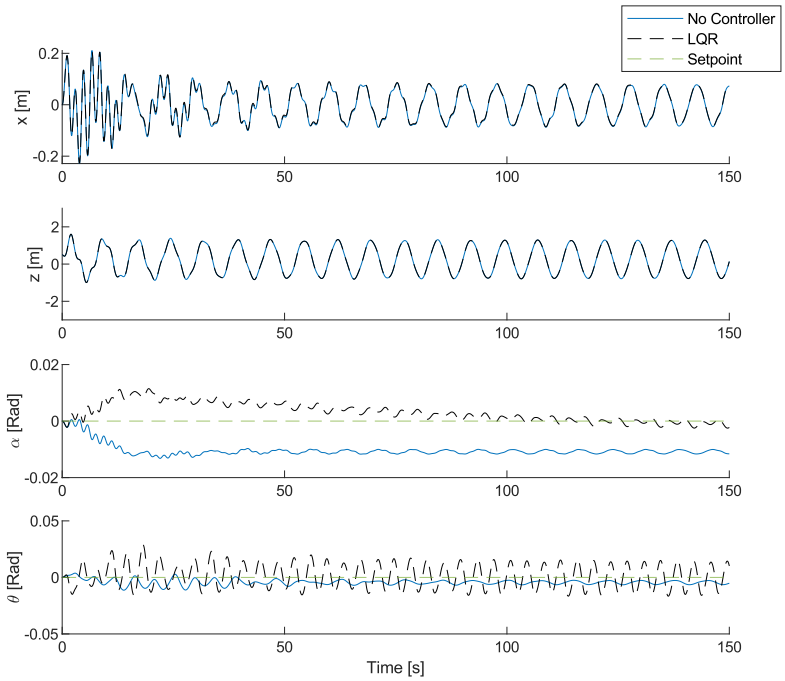

Figure 4.10: The system without a controller plotted against a system with an LQR controller, with ocean currents of -0.3 m/s, wave height H = 2, and peak period $T_0 = 9$.

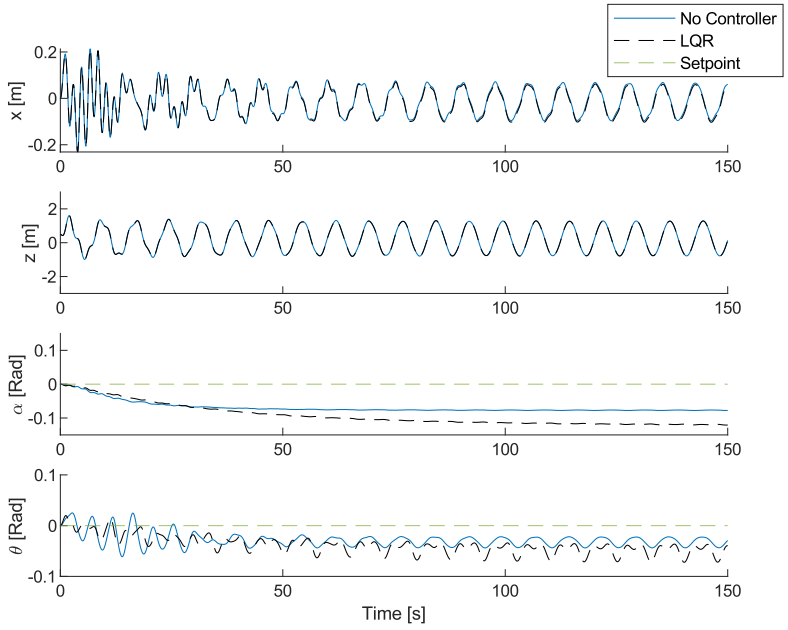

Figure 4.11: The system without a controller plotted against a system with an LQR controller, with ocean currents of -0.3 m/s, wave height H = 2, and peak period $T_0 = 9$.

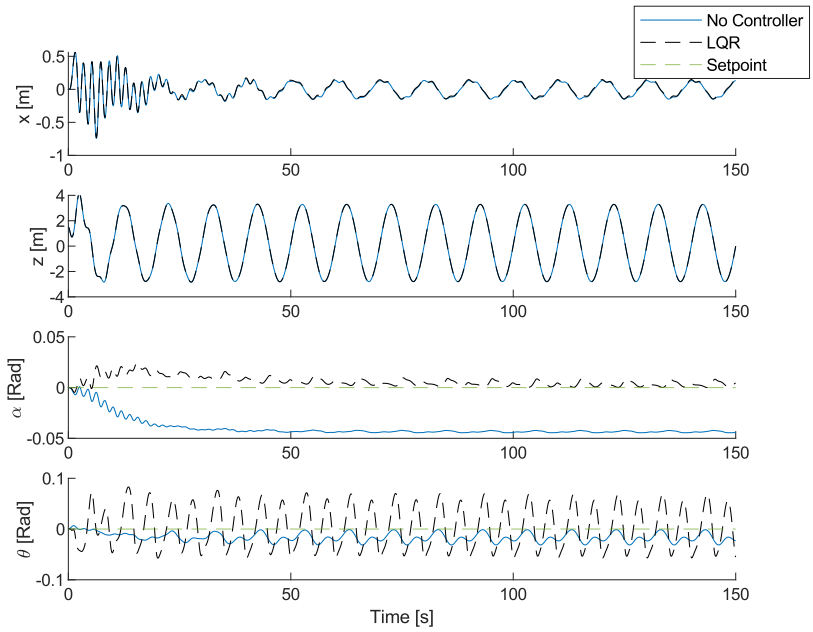

Figure 4.12: The system without a controller plotted against a system with an LQR controller, with ocean currents of -0.3 m/s, wave height H = 9, and peak period $T_0 = 14$.

4.6 JONSWAP System Simulation

We finish by simulating the system in a JONSWAP wave, figure 4.13 shows a simulation with an irregular wave. And what can be seen is that the randomness in the wave causes problems for the controller, as there are periods of the wave with low amplitude waves and visa-versa. This inconsistency makes α jump around the setpoint and causes oscillations in θ.

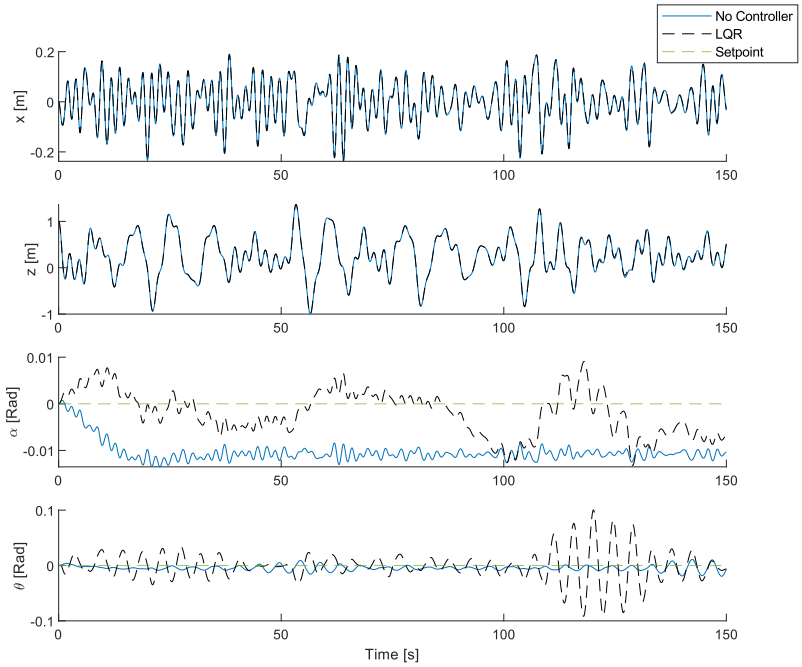

Figure 4.13: The system without a controller plotted against a system with an LQR controller, with ocean currents of -0.3 m/s, in a JONSWAP wave spectrum with $H_s = 2$, and peak period $T_0 = 9$.

Chapter 5

Discussion

We have implemented a model and controller in Matlab, simulated the results under different settings, and interpreted what this means for the system. Some thoughts about what the results could be interpreted as are given.

5.1 Model Accuracy

The choices made regarding the model, while done in the best effort, do have their limitations. A fully developed hydrodynamical model for the surface vessel in 6-DoF would need to be found once the shape and dimensions of the craft are finalized. We cannot be sure that diffraction and radiation forces affect the system's dynamics in a meaningful way. However, it is expected that those forces would not interact with the turbine dynamics significantly. Now the numerical results from the implementation of [10] against their experimental data suggest we should capture the main hydrodynamical forces in a good way, at least when looking at the configuration with a buoy. And that we observe behavior in our simulations in line with what is expected, considering wave drift forces are found that increase with wave magnitude.

One of the most significant part left out of the model is the force generated by the turbine blades and how that would affect the heave dynamic of the system, a proper model for the dynamic of the blades would be developed. While it does affect the heave speed profile of the turbine, it does not change the conclusion of the thesis. Another omission is that of the moment generated by the slightly different rotating speed of the two sets of turbine blades. The model could be updated to have yaw motion, but this is omitted here due to the increasing size of the equations of motion. As mention, the same is true for the different sized added mass. However, we get back to the moment generated by the turbines in a bit.

The most considerable uncertainty regarding the control system is the turbine's drag coefficient in surge, as this is the main force moving the turbine, however as it is taken of that of a cylinder. The turbine itself would, in likelihood, be more aerodynamic with a smaller drag coefficient and area.

5.2 Control System Implementation

While the systems LQR Controller achieves what it set out to be done, that is to contract the effects of the ocean currents quite well in some situations. It does have its shortcomings, most notably its dependence on ocean waves to work. As becomes especially clear when simulating with the JONSWAP wave spectrum, needing bigger wave amplitudes to work against greater currents, which can not be guaranteed. While at the same time, this provides a passive way to control the drift of the turbine, and some scenarios offer a more noticeable counter to the ocean currents. It does, however, come at the cost of more oscillations in the turbine pitch, θ.

5.3 Recommendations

When looking at the simulations done, it quickly becomes apparent that the turbine does not get displaced by a lot, even in conditions with high ocean currents. We are looking at horizontal displacement of at most 10 m, and that in current speeds up to 0.8 m/s. There are parts of the sea with currents at speeds higher than that, for instance, the gulf stream with speeds up to 2 m/s. Though, this approach would not work at such high speeds, as the drag created by such speeds would be far too high to be countered by the lift from the wings. And in parts of the sea where it would be natural to place the system as a part of a power plant, the ocean currents are significantly lower.

Therefore it is hard to see a benefit to adding the control system, at least in counteracting ocean currents. The added complexity of adding wings, motors to control the angle of attack of the wings, general electrical components such as sensors and micro-controllers would all add points of failure. And when the benefit is as low as this, it is hard to recommend implementing the system.

However, if it is found necessary to compensate for the momentum generated by the turbine blade rotation, this system could easily be modified to compensate for this. It could be done with the approach done in the prethesis project, where the wings' angle of attack is solved for optimal force distribution, with an updated model as mentioned previously.

Depending on the approach chosen, the wing area could be chosen rather freely. If the focus would be to counteract the moment, smaller wings with less drag could be chosen.

An exciting aspect could be to add two more wings for a 4 winged turbine, expanding on what is shown by figure 4.9, to help then the DP system keep the buoy in place. By adding the two extra wings, control could be achieved in 3-DoF compared to the 2 with the current set-up. It would then allow moving the buoy in both surge and sway, no matter what direction the ocean current flows in that area, and could lower the energy need of the buoys DP-system, allowing more energy to be stored up for low wave sea states.

5.4 Future Work

- A logical next step would be to see if possible to use some other way to counteract the ocean currents in more high-velocity scenarios. For instance, this could be done by adding a thruster in the bowl on the turbine while simply using a set of wings to steer counter the moment if needed. This solution would work in all scenarios and be in-depended on the ocean wave states.
- An updated hydrodynamical model should be developed when the surface buoy and turbine are finalized. At the same time, a proper model capturing the DP-system of the buoy should be added or a mooring model if looked at in the power plant setting, instead of the rudimentary solution used here. Also, a model in 6-DoF could be constructed from the same methods if deemed necessary
- It should also be looked into to develop a model for the turbine blades and their dynamics to see if the moment generated is significant and how this would affect the system.

Bibliography

[1] A. P. Trujillo and H. V. Thurman, *Essentials of Oceanography*. Pearson, 11 ed., 2014.

[2] A. Pecher and J. P. Kofoed, *Handbook of Ocean Wave Energy*, vol. 7 of *Ocean Engineering & Oceanography*. Cham: Springer International Publishing, 2017.

[3] K. H. Christensen, A. K. Sperrevik, and G. Broström, "On the variability in the onset of the Norwegian Coastal Current," *Journal of Physical Oceanography*, vol. 48, no. 3, pp. 723–738, 2018.

[4] P. M. Haugan, G. Evensen, J. A. Johannessen, O. M. Johannessen, and L. H. Pettersson, "Modeled and observed mesoscale circulation and wave-current refraction during the 1988 Norwegian Continental Shelf Experiment," *Journal of Geophysical Research*, vol. 96, no. C6, p. 10487, 1991.

[5] P. Fritzkowski and H. Kaminski, "Dynamics of a Rope as a Rigid Multibody System," *Journal of Mechanics of Materials and Structures*, vol. 3, pp. 1059–1075, 2008.

[6] H. Goldstein, C. P. Poole, and J. L. Safko, *Classical Mechanics: Pearson New International Edition*. Pearson, 3 ed., 2013.

[7] O. M. Faltinsen, *Sea Loads on Ships and Offshore*. Cambridge University Press, 1993.

[8] R. G. Dean and R. A. Dalrymple, *Water wave mechanics for engineers and scientists*. 1984.

[9] T. I. Fossen, *Handbook of Marine Craft Hydrodynamics and Motion Control*. Chichester, UK: John Wiley & Sons, Ltd, 2014 ed., apr 2011.

[10] Z. Ballard and B. Mann, "Experimental and numerical investigations of an untethered, nonlinear spherical buoy in a wave tank," *Proceedings of the ASME Design Engineering Technical Conference*, vol. 1, no. PARTS A AND B, pp. 429–437, 2011.

[11] D. Zhao, N. Han, E. Goh, J. Cater, and A. Reinecke, *Wind turbines and aerodynamics energy harvesters*. Academic Press, 1 ed., 2019.

[12] B. Sumer and J. Fredsøe, *Hydrodynamics Around Cylindrical Structures (Revised Edition)*, vol. 26. World Scientific Publishing Co Pte Ltd, 2006.

[13] "DNV-RP-H103 Modelling and Analysis of Marine Operations. Recommended practiceAS, D. N. V. (2011). DNV-RP-H103 Modelling and Analysis of Marine Operations. Recommended practice.," tech. rep., 2011.

[14] J. Katz and A. Plotkin, *Low-Speed Aerodynamics*. Cambridge University Press, 2. ed., feb 2001.

[15] J. Hespanha, *Linear Systems Theory*. Princeton: Princeton University Press, 2009.

[16] DNV-GL, "Class Guidline - Wave Loads (DNVGL-CG-0130)," tech. rep., 2018.

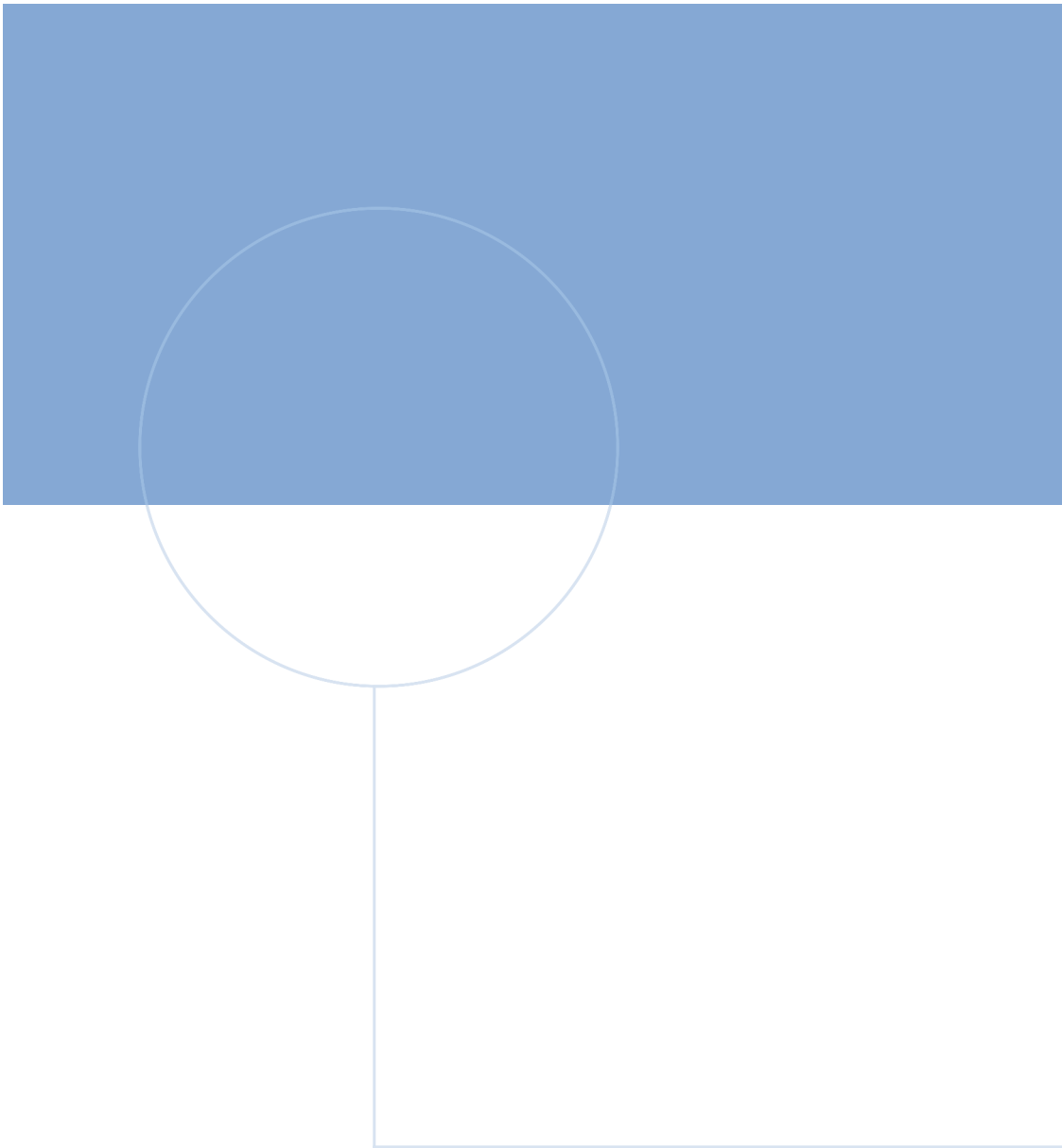

NTNU

Norwegian University of
Science and Technology